

# Thermal Science and Engineering Progress

## Early detection of the breast cancer using infrared technology – A Comprehensive Review --Manuscript Draft--

<b>Manuscript Number:</b>	TSEP-D-20-00638R1
<b>Article Type:</b>	Review Article
<b>Keywords:</b>	Thermography; Breast cancer; Numerical modeling; Reverse modeling; Artificial Intelligence; Machine Learning
<b>Corresponding Author:</b>	Aigerim Mashekova, PhD Nazarbayev University KAZAKHSTAN
<b>First Author:</b>	Aigerim Mashekova, PhD
<b>Order of Authors:</b>	Aigerim Mashekova, PhD Yong Zhao, PhD Eddie Yin Kwee Ng, PhD Vasileios Zarikas, PhD Sai Cheong Fok, PhD Olzhas Mukhmetov, MSc
<b>Abstract:</b>	<p>Breast cancer is one of the most common and fatal ailments among women that can also affect men. Early detection and treatment of this disease can increase the chances for recovery. Currently there are many different breast cancer screening approaches, each of which having its own advantages and disadvantages. Thermography is one of such breast cancer screening methods characterized as safe and non-invasive. The approach with emerging image processing and intelligent classification techniques has gained renewed interests. The non-contact technology, which is relatively inexpensive, has great potential to be integrated with the Internet for the early detection of breast cancer through mass screening and subsequent continuous monitoring of suspicious patients. This paper presents a comprehensive review of previous studies conducted at the nexus of thermography, numerical simulation and artificial intelligence that can enhance early detection of breast cancer.</p>
<b>Suggested Reviewers:</b>	Natteri Sudharsan, PhD Professor, Rajalakshmi Engineering College sudharsann@asme.org  Wong Teck Neng, PhD Associate Professor, Nanyang Technological University Mtnwong@ntu.edu.sg  Yubing Shi, PhD University of Northampton Yubing.Shi@northampton.ac.uk
<b>Response to Reviewers:</b>	

Dr Aigerim Mashekova  
Nazarbayev University  
53 Kabanbay batyr avenue  
Nur-Sultan, Kazakhstan  
aigerim.mashekova@nu.edu.kz

Editor-in-Chief  
Journal of Thermal Science and Engineering Progress

August 23, 2020

Dear Editor-in-Chief,

I am pleased to submit review article entitled “*Early detection of the breast cancer using infrared technology – A Comprehensive Review*”. The review was conducted by a group of researchers of Nazarbayev University together with prof. Michael Yong Zhao, prof. Eddie Yin Kwee Ng, and prof. Sai Fok. The paper is submitted for your consideration for publication in *Journal of Thermal Science and Engineering Progress*.

This manuscript includes:

- historical development of the thermography as an additional tool for the breast cancer detection;
- overview of the bioheat transfer equation and the geometrical models of the breast development, used for the numerical modelling of the process of breast cancer detection based on the thermography;
- overview of the numerical simulation studies for the breast cancer detection, that helps to quantify the methods of breast cancer detection;
- overview of the Artificial Intelligence (AI) methods and techniques for early breast cancer detection;
- highlights of the problems of the thermography and its further development using the numerical simulation and AI.

We believe that this manuscript is appropriate for publication by *Journal of Thermal Science and Engineering Progress* because one of the topics of the journal is thermal biological and medical systems, as well as rapid development in engineering being made in thermal transfer processes. The paper presents a review of the thermography development and its recent connection with the mathematical modeling and AI that coincides with the scope of the journal.

This manuscript has not been published and is not under consideration for publication elsewhere. We have no conflicts of interest to disclose.

Thank you for your consideration!

Sincerely,  
Aigerim Mashekova, PhD  
Research Fellow

Manuscript Number: TSEP-D-20-00638

# Early detection of the breast cancer using infrared technology – A Comprehensive Review

## Replies to the comments of the reviewers

Reviewer 1		
	Comments	Replies
1	As the manuscript claimed to present a detailed survey on the applications of thermal imaging, a well-organized presentation has been expected. The paper fails in the presentation. The manuscript provides several vital information regarding thermography in detection of breast cancer, but the representation is very poor. The manuscript is not readable at all, it contains critical grammatical errors and typos.	According to the comments given, the manuscript has been thoroughly revised and improved. Totally revised parts of the paper indicated by yellow.
2	Low quality figures are used in the manuscript. The figures are not understandable.	Figures 4b, 5a and 5b were replaced with high quality ones.
3	The mathematical formulations and geometrical representation of the breast related to the applications of thermal imaging is described elaborately. Table-1 and Table-2 are representing good summary on the mathematical models and breast geometry. But the observations from the tables are not stated clearly.	<p><b>We have improved the description for Table 1 (changed to Table 2) as follows in the text:</b></p> <p>The biothermal mathematical equations presented in Table 2 can be described in terms of two main approaches: continuum and discrete-vessel models. The continuum model is the simplified type of biothermal equations, which describe the effects of the blood flow on the temperature distribution by considering the average blood supply over the average volume in the area of interest. The continuum approach was used in the works of Pennes [50] and Wulff's energy conservation equation [61].</p> <p>The discrete-vessel model is a more advanced and sophisticated approach, which is based on biothermal equations describing the blood flow in each individual vessel in the area of interest. This approach was described in the works of Mitchell and Myers [36], Keller and Seiler [39], Chen and Holmes [40], as well as Weinbaum-Jiji-Lemons, which included a simplified version of their model [62-69].</p> <p>Commonly used idealized mathematical models of Pennes and Wulf neglect such effects as heat transfer between blood and tissue, the blood flow, as well as the size of the blood vessels and their location relative to each other. Pennes' equation has a reasonable agreement with the experimental data and is often used to describe temperature distribution in the area of interest. The more sophisticated</p>

	<p>discrete-vessel model takes into account detailed information about the network vessel and blood perfusion. The approach takes into consideration the existence of temperature difference between arteries and veins, which are close to each other, and the heat transfer that occurs in opposite flow between them. The approach requires a set of biothermal equations describing the movement of blood in each individual blood vessel. Countercurrent flow is also considered and this has a significant impact on the heat transfer equilibrium. As a result, the temperature distributions can be predicted with higher resolutions in the adjacent tissues of interest. In particular, the mathematical model of Weinbaum-Jiji-Lemons can describe the heat transfer in the acentric tissues, where its assumptions are valid. Anatomy and vessel geometry data is needed in the application of the model. The data includes the density of the vessel, the size and distance between artery and vein, as well as blood perfusion rate.</p> <p>Many researchers used these mathematical models to study the effect of the blood flow and diameter of blood vessels on the temperature distributions. According to Chato et al. [41] higher blood flow decreases upon downsizing of the blood vessel, and therefore the heat transfer coefficient can be determined in countercurrent flow. Charny and Levin [70] studied the heat transfer between the artery and vein, and showed that thermal equilibrium of the system can be reached at the distance of 43 mm from the main vessels. In addition, it was established that the countercurrent flow can reduce the temperature of the tissue by 0.5 °C. These works illustrated the applicability of mathematical models. The choice of appropriate biothermal model should be based on the objectives of the study and specific biophysics features of the cases.</p> <p><b>The description for Table 2 (changed to Table 3) has also been revised as follows:</b></p> <p>Table 3 lists the studies that used different breast geometries and predictive models to relate the temperature distributions to the tumor sizes, locations, metabolic heat generation and blood perfusion rates. Four main types of the breast geometries were developed in these studies [74-85]: rectangular, hemispherical, deformed hemisphere and patient-specific.</p> <p>Osman and Afify [74, 75] developed a 2D multilayer breast geometry in 1984. The work was extended in 1988 using a 3D breast geometry to estimate the influence of the size and location of the tumor on the temperature distribution of the breast surface. This model was not used by other researchers as it creates high temperature differences in the layers close to the surface [86].</p>
--	---

	<p>Further studies by Ng and Sudharsan [76, 77] led to improvement in both 2D and 3D multilayer breast models. They made 3D flexible models with tissue layers of different thicknesses and separated the geometry into four quadrants to investigate the temperature differences in the upper-outer, lower-outer, as upper-inner, and lower-inner segments. This model was widely adopted in many studies in the determination of the effects of different tumour parameters on the thermal distributions.</p> <p>Gonzalez [78] used a hemisphere breast model and added a thick layer of 1.3 cm to simulate the chest wall. The results of the study revealed that Finite Element Simulations are able to detect 3 cm tumors located at the depth of 7 cm from the surface. Bezerra et al [79] modelled the breast geometry based on the silicone prostheses. The cylindrical geometry was improved with nodule type, size, depth and location extracted from an ultrasound examination of a patient. The study established the methodology to define the thermophysical properties of the breast tissues and nodules using maximum temperature from the temperature profile. Das and Mishra [80] in 2013 used a rectangular domain, single layer breast model with the Pennes' bioheat equation to diagnose a tumor based on the temperature distribution on the surface of the breast. The rectangular model does not reflect the real shape of the breast and it was difficult to validate the results with thermograms. As a result, no concrete conclusion was drawn. The authors later created a single layer 3D hemispherical model with a tumor [81], and found that the developed tool could be used not only to detect small tumors closed to the surface of the breast, but also big tumors located deep inside the breast, when there is a clear temperature difference on the surface of the breast. Amri et al. [82] used a 3D rectangular breast model to conduct steady-state and transient numerical simulations. Their results showed that the rewarming process after applying the cold stress gave more information about the tumor. However, the main problem with the rectangular breast models is that it did not correlate to the real breast geometry and its tissue layers. In addition, such breast geometry employed uniform properties for the tissue and tumour, which could not be validated by experiments.</p> <p>There are many studies based on the rectangular and spherical computational domains, but very little technical literature on the use of personalized patients' breast geometries in numerical investigations. Mukhmetov et al. [73] created 3D numerical models by scanning a mannequin and real patients' breasts. The obtained numerical findings were validated by experiments using artificial and human breasts. Aitbek et al. [85] enhanced patients' specific model by creating different layers inside the breast and estimated the influence of the fat on the</p>
--	--

		temperature distribution on the surface of the breast and thereby identify the tumor inside the breast.
4	A large number of researches have conducted in the field of machine learning for implementing CAD based breast cancer detection systems. The manuscript failed to provide satisfactory reviews on these area. Few critical information such as how Hotspot area is related to the tumor area etc.. are not mentioned.	Thanks for the comments. We aim to provide a comprehensive and also balanced review on the latest developments in the following: physics-driven analysis and diagnosis and data-driven analysis and diagnosis and their possible integration. We have provided detailed review on them, but we can not dedicate the whole paper to one of them as they are all promising techniques. In fact we believe the integration of the two techniques would be even more promising and we are working on a project for such integration.
<b>Reviewer 2</b>		
	<b>Comments</b>	<b>Replies</b>
1	Referencing is in both square [] and () could you please check the style for consistency.	We have changed all of them to Square brackets for referencing
2	Page 2 Line 6 In 2016, there were 246,660 cases of breast cancer identified in the United States This is 5 years ago. A table with current statistics based on different continents would help.	<b>The statistics was updated as follows:</b> Breast cancer is one of the commonly occurring types of cancer. According to the World Health Organisation (WHO), there were 2.3 million new cases of breast cancer identified among the women worldwide in 2020. Furthermore, in the past five years (2016-2020), there were 7.8 million women alive who were diagnosed with breast cancer, making it the world's most prevalent cancer. At the same time, as the WHO reports, the number of deaths caused by breast cancer in this period equals to 685,000. This number is less than the one caused by other types of cancer such as lung (1.8 millions deaths), liver (830 thousands deaths), and stomach (769 thousands deaths). This allows us to suppose that breast cancer is more treatable if it is diagnosed at an early stage. Early detection of the tumour includes the ones determined at the stages 0, 1 and 2. These stages are classified by the diameter of the tumour or its spread to the nearby lymph nodes [4, 5]. Therefore, precise and early diagnosis plays an important role in successful treatment of breast cancer and has generated tremendous interests [5, 6].
3	Page 3 Line 26 About the IR Device Need explain in terms of Noise Equivalent Temperature Difference (NETD), IR resolution and Thermal Sensitivity. Also a table with various IR Cameras suitable for biological imaging (8 - 12 micrometer wavelength) should help researchers in identifying the best device.	Thanks for the comments. So far, details of the IR devices used by various researchers are difficult to find out. The majority of manufacturers also do not provide information on NETD. They may provide information on resolution/sensitivity and accuracy. We have added a table that lists various IR Cameras suitable for biological imaging in the article.  Table 1. List of infrared cameras


			Flir T560-EST	down to -40°C	640 × 480	<40 mK @ 30°C (86°F)	7.5 – 14 μm	±1°C / ±1%	universal	thermal imaging
4	page 3 Line 52 It was obtained that the accuracy of the steady state thermography was 54%, whereas the accuracy of the dynamic infrared thermography was equal to 82%. I think this term accuracy is to do with False positive and negative rather as I feel that the term accuracy is more specific to the device being used.	Thanks for the comment. We corrected the text. We refer to the diagnostic accuracy and not the instrument accuracy. In both papers [52] and [53] that we cited and discussed, the authors reported the diagnostic accuracy. The accuracy for the simple case of a diagnosis with two states, Negative and Positive, is defined by: Accuracy= (TP+TN)/(TP+FP+TN+FN).								

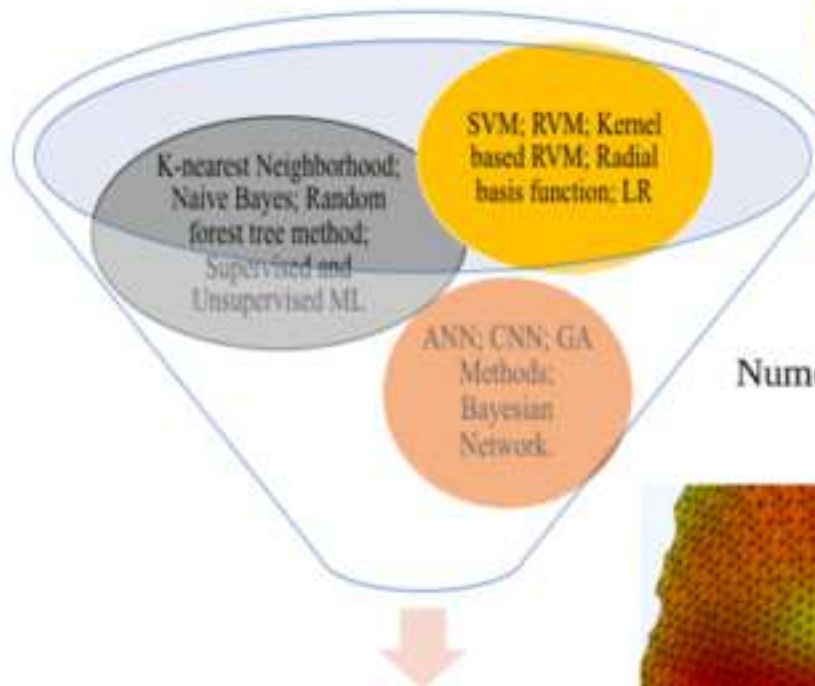


### Highlights of the paper

1. Overview of the mathematical basis and historical development of the thermography as a supplementary technique for the breast cancer detection;
2. Overview of the numerical simulation development for breast cancer detection and mathematical basis of the bioheat transfer equation, employed as supplementary tool for thermography;
3. Overview of the methods and techniques of the Artificial Intelligence that were used to detect breast cancer based on the obtained thermograms;
4. Highlights of the thermography and numerical simulations problems to detect breast cancer;
5. Further development of the thermography as a supplementary tool for early breast cancer detection using numerical simulations and Artificial Intelligence.

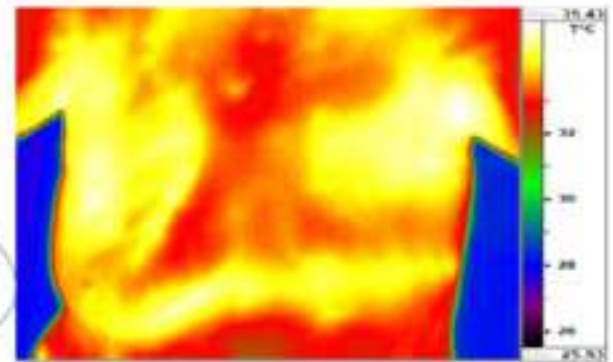
# REVIEW

## Methods and Techniques of Artificial Intelligence

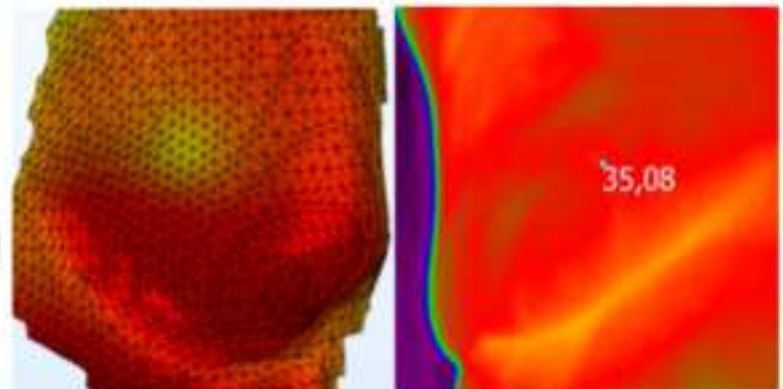


Breast Cancer Detection based  
on Thermography

## Development of Thermography for breast cancer detection



## Numerical Simulation basics for breast cancer detection



# Early detection of the breast cancer using infrared technology – A Comprehensive Review

Aigerim Mashekova<sup>1</sup>, Yong Zhao<sup>1</sup>, Eddie Y.K. Ng<sup>2</sup>, Vasileios Zarikas<sup>1</sup>, Sai Cheong Fok<sup>1</sup>,  
Olzhas Mukhmetov<sup>1</sup>

<sup>1</sup>Nazarbayev University, School of Engineering and Digital Sciences, Nur-Sultan, Kazakhstan

<sup>2</sup>Nanyang Technological University, School of Mechanical and Aerospace Engineering, Singapore

\*corresponding author: [aigerim.mashekova@nu.edu.kz](mailto:aigerim.mashekova@nu.edu.kz), 53, Kabanbai batyr street, Nur-Sultan, Kazakhstan

Emails: [yong.zhao@nu.edu.kz](mailto:yong.zhao@nu.edu.kz), [MYKNG@ntu.edu.sg](mailto:MYKNG@ntu.edu.sg), [vasileious.zarikas@nu.edu.kz](mailto:vasileious.zarikas@nu.edu.kz),  
[scfokky@yahoo.com.au](mailto:scfokky@yahoo.com.au), [olzhas.mukhmetov@nu.edu.kz](mailto:olzhas.mukhmetov@nu.edu.kz)

## Abstract

Breast cancer is one of the most common and fatal ailments among women that can also affect men. Early detection and treatment of this disease can increase the chances for recovery. Currently there are many different breast cancer screening approaches, each of which having its own advantages and disadvantages. Thermography is one of such breast cancer screening methods characterized as safe and non-invasive. The approach with emerging image processing and intelligent classification techniques has gained renewed interests. The non-contact technology, which is relatively inexpensive, has great potential to be integrated with the Internet for the early detection of breast cancer through mass screening and subsequent continuous monitoring of suspicious patients. This paper presents a comprehensive review of previous studies conducted at the nexus of thermography, numerical simulation and artificial intelligence that can enhance early detection of breast cancer.

**Keywords:** thermography, breast cancer, numerical modeling, reverse modeling, artificial intelligence, machine learning

## 1. Introduction

Cancer is a term that defines a number of disorders related to uncontrolled cell mutation as a result of tumor upraise [1]. Commonly, tumors may occur in such organs as skin, lung, prostate, breast, and pancreas. There are no exact factors that influence the spread of such ailment, however, most of the experts agree that unhealthy lifestyle, alcohol consumption, smoking, ultraviolet radiation, influence of carcinogenic agents, age, and genetic predisposition are some common causes of tumor origination [2, 3].

Breast cancer is one of the commonly occurring types of cancer. According to the World Health Organisation (WHO), there were 2.3 million new cases of breast cancer identified among the women worldwide in 2020. In the past five years (2016-2020), there were 7.8 million women alive who were diagnosed with breast cancer, making it the world's most prevalent cancer. WHO reported that the number of deaths caused by breast cancer in this period equals to 685,000. This number is less than the deaths due to other types of cancer such as lung (1.8 millions deaths), liver (830 thousands deaths), and stomach (769 thousands deaths) [4, 5]. This indicated that breast cancer is treatable. At present, breast tumors are diagnosed by the stages of tumor development, which can be classified by the tumor diameter or its spread to the nearby lymph nodes [4]. Precise and early diagnosis plays an important role in the successful treatment of the disease and this has generated tremendous interests [5, 6].

Most of the studies on the diagnosis of breast cancer focused on mammography, ultrasound and Magnetic Resonance Imaging (MRI). These approaches are recognized as the gold standard techniques. However, their limitations, such as lack of access for cancer detection in rural and remote areas, led to the development of alternative technologies: electronic palpation imaging, electrical impedance scanning

(EIS), and thermal imaging (thermography) [1]. This paper focuses on thermography as it is one of the cheapest, non-invasive, radiation free and prospective techniques.

Thermography (a.k.a. infrared imaging) uses infrared (IR) cameras to map the temperature profiles of the breast. Hence, the existence of a tumor is based on the temperature distribution on the breast [7, 8, 9]. The main principle of the IR image diagnosing is that unregulated growth of cells generates higher metabolic rate and requires more blood perfusion, in comparison to the surrounding tissues. Extra generated heat dissipates to the tissue around the tumor, and thereby causes the temperature spike on the breast surface. This temperature spike is observed by using IR imaging to detect the tumor [7, 8, 9].

The diagnosis of breast cancer using surface temperature of the breast is based on the identification of specific features of the breast's heat patterns over time. The most common features include: 1) highly asymmetric temperature distributions between the left and right breasts (i.e. based on the assumption that one is healthy and the other is not); 2) localized hot spots indicating abnormalities; 3) changes in hypothermic vascular patterns due to tumor growth; 4) variation of heat patterns in the areolar and periareolar areas [10, 11, 12].

It is important that the breast size and geometry as well as physiological conditions such as menstruation, stress and anxiety, hormone intake (contraceptive), pregnancy and lactation should be taken into account when making a decision, as sometimes a temperature difference of 2 °C between the cooler and warmer regions, and between asymmetric areas of two breasts can be considered as normal, while a difference from 1 °C to 2.5 °C can be considered as suspicious [8, 13, 14].

The following sections discuss breast cancer detection with IR imaging and computer technology.

## 2. Breast Thermography

The basics of thermography came from earlier studies by Hardy [15, 16, 17], Hardy and Muschenheim [18, 19], Clark, Vinegar and Hardy [20], Hardy, Hammel and Murgatroyd [21], Derksen, Monahan and Lawes [22], Mitchell [23], Quinn [24], Watmough [25], Steketee [26], Quinn and Compton [27], Pratt [28], as well as Andersen and Parrish [29], who concluded that IR cameras can produce reliable measurements of the actual temperatures. They observed that skin emissivity is about  $0.989 \pm 0.01$  and does not depend on the wavelength, whereas the connection of the spectral radiance with the wavelength can be described by the Planck's radiation law, where the intensity of the electromagnetic radiation ( $B$ ) is a function of wavelength ( $\lambda$ ) and temperature of the object ( $T$ ), as described by the following equation:

$$B_{\lambda}(\lambda, T) = \frac{2hc^2}{\lambda^5} (e^{\frac{hc}{\lambda kT}} - 1)^{-1} \quad (1)$$

where  $B(\lambda, T)$  - radiation power;  $h$  - the Planck constant,  $c_s$  - the speed of light in vacuum, and  $k$  - the Boltzmann constant.

Thermography was used for the first time in 1956 to diagnose breast cancer [30]. Further research by Lawson and Chughtai found that the temperature difference of the same area between healthy and diseased breasts is about 2°C [31]. The same results were obtained by Gautherie [32] in 1980, who used a fine needle thermocouple to measure temperature inside the breast with malignant tumor. Other studies [2, 12, 14 - 31, 33 - 42] revealed similar results, which showed that the existence of the tumor inside the breast leads to higher temperature showing up as a hotspot on the thermogram. In 1982, thermography was approved as a supplementary tool to mammography for breast cancer diagnosis in the US.

Further development of infrared thermography for the breast tumour detection had some successes and drawbacks. In a clinical study conducted by Gamagami [43], it was reported that 15% of non-palpable cancers went undetected by mammography, but were detected by IR thermography. Gautherie and Gross [12, 44] studied 1245 patients who had abnormal IR image profiles and found that 35% of the patients with abnormal thermograms developed cancer within the next 5 years. They found that IR imaging may be suitable for the early detection of breast cancer and rapidly growing neoplasms. However, the approach was not able to differentiate the cancerous region of the breast and inflammation zones. In addition, the false positive results of breast cancer were high [32]. The rate of true positive diagnosis was as low as 41%.

This was attributed to both the measurement process and the equipment. Most clinicians were neither familiar with nor adequately trained in using IR cameras and there was a lack of measurement standards [32]. On top of that, poor camera resolution and scan time also affected the usefulness of the approach at that time. Chen et al. [35] observed that the specification of the cameras is limited, as the typical resolution was low with a scan time of 4 seconds. Such specification was not suitable for detecting deep tumors, only shallow tumors could be diagnosed. The reason is that the temperature pattern of the healthy and tumorous breast with deep tumor inside could be very subtle. These issues impede the popularity of IR thermography as a method of earlier breast cancer detection [12, 44, 45, 46].

In the 2000s IR cameras have significantly improved their performance, especially when used together with black body, and nominal accuracy could be varied from 0.1 - 1 °C and scan time of 0.8 seconds (Table 1). Such improvement in the performance of cameras allowed them to detect deeper tumors, and observed less distinguished temperature variations on the surface of the breast. This also leads to the development of breast tumor detection methods, such as dynamic infrared thermography (DIT). The method aims to capture the thermal contrast between cancerous and non-cancerous regions during the rewarming of the breast after the application of cold stress. The principle is based on the fact that the temperature patterns of the cancerous region in the breast remain the same, while those of the healthy regions are affected by cold stress. Similarly the cancerous breast has different temperature patterns from those of a healthy breast under cold stress. In fact the studies conducted by Usuki et al. [47], Cockburn [48] and Mooibroek et al. [49] observed that tumors produce a chemical mediator under thermal stress. This chemical dilates the subcutaneous vessels and enhances the contrast in temperature differences between the tumor and the surrounding region [50]. The magnitude of the reaction to the thermal stress can vary depending on the tumor size. The effects of cold stress on different tumor sizes need to be thoroughly investigated. According to Gullino [51], the tumor vessels' response to cold stress can be insignificant for deeper tumors.

Table 1. List of selected infrared cameras for medical applications

	Measuring range	Resolution (pixels)	Thermal sensitivity	Spectral range	Temperature measurement accuracy	Application	Function
Micro-Epsilon	-20 °C to 100 °C	382 × 288	40 mK	7.5 – 13 μm		fever screening; medical	thermal imaging, measuring
IRTIS 2000	-60°C - +300°C (+1700°C)	320 (640) × 240 (480)	0,05° C (0.02° C)	3 – 5 (8 – 12) μm	±1% or ±1°C	medical	thermal imaging

Fluke Ti480 PRO Infrared Camera	$\leq -20^{\circ}\text{C}$ to $1000^{\circ}\text{C}$	$640 \times 480$	50 mK	$7.5\text{ }\mu\text{m}$ to $14\text{ }\mu\text{m}$ (long wave)	$\pm 2^{\circ}\text{C}$ or 2% (at $25^{\circ}\text{C}$ nominal, whichever is greater)	universal	thermal imaging
Hikvisio n CA- DS- 2TE127- G4A	$5^{\circ}\text{C} - 50^{\circ}\text{C}$	$160 \times 120$	Less than 40 mK	8 – 14 $\mu\text{m}$	$\pm 0.1^{\circ}\text{C}$	medical	thermal imaging
Flir T560- EST	down to - $40^{\circ}\text{C}$	$640 \times 480$	<40 mK @ $30^{\circ}\text{C}$ ( $86^{\circ}\text{F}$ )	$7.5 - 14\text{ }\mu\text{m}$	$\pm 1^{\circ}\text{C} / \pm 1\%$	universal	thermal imaging

One of the major studies, conducted in the field of DIT, was carried out by Ohashi and Uchida [52], which included 728 cases of breast cancer, with thermograms from both steady state and dynamic infrared imaging. During the experiments the ambient temperature was maintained at  $21^{\circ}\text{C}$  and a fan was applied for 2 minutes for the dynamic infrared thermography. The diagnostic accuracy of the steady state thermography was 54%, whereas the diagnostic accuracy of the dynamic infrared thermography was equal to 82%, see [52]. A similar DIT method for the increase of the diagnostic accuracy of melanoma, was developed in [53]. In this work it was emphasized that to perform steady state thermography properly, there are strict requirements for the environmental conditions of the room, as well as adequate time for the patient to adapt to the room temperature. Dynamic infrared thermography does not require such strict conditions for the room and is quicker as well as more effective in the generation of the thermal contrast between the tumor and the surrounding healthy tissues. To further improve the performances of DIT using modern IR detectors, Ng [45] suggested minimizing the sources of IR interference. Minimization of undesirable interference can be achieved using a plain, nonreflective background, covering IR reflective surfaces, and blocking of sunlight through windows as well as from incandescent or halogen light sources. The main drawback of the dynamic infrared thermography is that there is no standardized and systematic approach. Accurate and meaningful results depend on the size and depth of the tumor. Another main concern of dynamic infrared thermography is the patient discomfort during the application of the cold stress, as the cooling duration can last between 2 and 6 minutes at temperatures below  $15^{\circ}\text{C}$  [54, 55]. Results from different studies have very high variation of accuracy for dynamic thermography, therefore even if its accuracy is high, it is not preferred to be used in practice.

Many researchers had examined the prognostic aspects of infrared thermography for the detection of breast cancer. Isard et al [37, 56] conducted a study with 10,000 breast thermograms over four years before recommending thermography as an adjunct tool for mammography, rather than an independent tool for breast cancer detection. It was found that among the 1,000 cases examined by both thermography and mammography, 45% of the thermograms were found to be abnormal and 21.4 % were eventually validated to be cancerous by mammography. In another study with 70 patients, who were followed up from 6 years



to 13 years, Isard concluded that thermography could be a prognostic indicator of survival. Gautherie and Gros [12] found that patients with abnormal thermograms had higher risk of developing breast cancer later. Another study [57] found that thermographic results were strongly correlated with the prognostic indicators of tumor growth, such as: the concentration of ferritin in the tumor, proportion of cells in DNA synthesis and proliferating, expression of the proliferation-associated tumor antigen Ki-67. Therefore, the patients with abnormal thermograms had faster growing tumors, which could be indicated in the thermograms. The conclusion was based on the results of 100 normal patients, 100 living cancer patients and 126 deceased cancer patients. Study by Guidi and Schnitt [58] found a strong correlation between the number of vessels and further spread to the metastatic disease.

Most of the studies recommended thermography as an additional tool to complement mammography. The finding was also supported in recent research by Omranipour et al [59], who compared true positive rate (TPR), true negative rate (TNR), positive predictive value (PPV) and negative predictive value (NPV) of thermography and mammography. The results for the mammography were: TPR 80.5%, TNR 73.3%, PPV 85.4%, NPV 66.0%; in contrast the results for thermography were: TPR 81.6%, TNR 57.8%, PPV 78.9% and NPV 69.7%. These findings confirmed that thermography can complement but not substitute mammography for the early detection of breast cancer. The U.S. Food and Drug Administration (FDA) also does not recommend thermography to be used as a standalone tool for breast cancer detection, but suggested that it can be used as an additional tool with another diagnostic technique [60]. This could be due to the drawbacks of the approach. Thermography is very sensitive to the temperature and wellness of the patient. In addition, the approach is prone to procedural errors including incorrect positioning of the breast, inability to eliminate nearby heat source emission and difficulties in maintaining a suitable distance between the IR camera and the patient. These errors led to poor thermal images with hidden areas especially for large breasts with fatty tissues.

### 3. Numerical thermal simulation of breast cancer

#### 3.1 Mathematical equations

Heat transfer in living tissues is a complex thermal process, which consists of the metabolic heat generation, heat conduction and blood perfusion. In regard to breast cancer diagnosis, a number of studies have developed mathematical models to describe the heat transfer behavior and to predict temperature distributions of the breast tissues, and the existence of a tumor inside the breast. Table 2 presents the main studies and mathematical models of each approach in the studies.

Table 2. Main studies and its mathematical models

Authors	Equation	Meaning
Pennes, 1948 [50]	$\rho_{ti}c_{ti}\frac{\partial T}{\partial t} = \nabla \cdot (k_{ti}\nabla T) - \omega_b c_b (T - T_{art}) + q_m$ <p>where</p> <p><math>\rho_{ti}</math> - tissue density; <math>c_{ti}</math> - tissue specific heat; <math>k_{ti}</math> - tissue thermal conductivity; <math>c_b</math> - blood specific heat; <math>T</math> - temperature; <math>q_m</math> - heat generations due to metabolism; <math>\omega_b</math> - blood perfusion rate; <math>T_{art}</math> - arterial blood temperature; <math>ti</math>, <math>b</math>, <math>art</math> - subscripts indicating tissue, blood, artery, respectively</p>	Commonly used equation based on the Fourier's law, considering the thermal energy equilibrium: alignment of the temperature in the tissue depending on the external and internal heat sources

<p>Mitchell and Myers, 1968 [36]</p>	$(1) \quad mc \frac{dT_{art}}{dx} + (UA')_v (T_{art} - T_v) + (UA')_{art} (T_{art} - T_\infty) = 0$ $(2) \quad -mc \frac{dT_v}{dx} + (UA')_v (T_v - T_{art}) + (UA')_{art} (T_v - T_\infty) = 0$ $(3) \quad x = 0: T_{art} = T_0; x = L; T_{art} = T_v$ <p><math>U</math> - thermal conductance; <math>A'</math> - heat transfer area per length; <math>\Delta T</math> - temperature difference causing the heat flow; <math>T_v</math> - vein blood temperature; <math>v</math> - subscripts to indicate vein</p>	<p>One of the first equations in the discrete-vessel approach, where the first equation describes the arterial flow, the second equation indicates the venous flow, and the last equation represents the temperature boundary conditions</p>
<p>Keller and Seiler, 1971 [39]</p>	$k_{ti} \frac{d^2 T}{dx^2} + (ha + c_h \dot{g})(T_{art} - T) + ha(T_v - T) + q_m = 0$ $\left[ (\dot{m}_{art})_0 - \int_0^x \dot{g} dx \right] c_h \frac{dT_{art}}{dx} + ha(T_{art} - T) = 0$ $\left[ (\dot{m}_{art})_0 - \int_0^x \dot{g} dx \right] c_h \frac{dT_v}{dx} + (ha + c_h \dot{g})(T - T_v) = 0$ <p>with the following boundary conditions</p> $x = 0, T = T_{art} = T_b; x = \delta, T = T_v = T_s$ <p>where</p> <p><math>x</math> - length in the direction of normal to surface, <math>h</math> - average coefficient of heat transfer from vessels to tissues, <math>a</math> - average area for heat transfer per unit volume, <math>c_h</math> - heat capacity, <math>g</math> - capillary perfusion rate, <math>m</math> - blood flow rate, <math>S</math> - thickness of tissue layer; <math>s</math> - subscripts to indicate skin</p>	<p>Extension of the biothermal set of equations of Mitchell and Myers by adding conservation of the energy in the surrounding tissues of veins and capillaries in the area of interest. The influence of the perfusion rate of the capillary on thermal transfer in subdermic area is included</p>
<p>Wulff, 1974 [61]</p>	$\rho_{ti} c_{ti} \frac{\partial T}{\partial t} = \nabla \cdot (k_{ti} \nabla T) - p_b c_b U_h \cdot \nabla T + q_m,$ <p>where</p> <p><math>\rho_b</math> - blood density; <math>U_h</math> - metabolic reaction enthalpy</p>	<p>Mathematical model of the equilibrium of the blood and tissue temperatures, as well as the value of the metabolic reaction <math>(p_b c_b U_h \cdot \nabla T)</math>,</p>



		which equals to $q_m$
Chen and Holmes, 1980 [40]	$p_{ti,eff} c_{ti,eff} \frac{\partial T}{\partial t} = \nabla \cdot (k_{ti} \nabla T) + p_b c_b w_b \cdot (T_{art} - T) - p_b c_b v \cdot \nabla T + \nabla \cdot k_p \nabla T + q_m,$ <p>where</p> $\rho_{ti,eff} = (1 - \varepsilon_{t,p}) \rho_{ti} + \varepsilon_{t,p} \rho_b$ $c_{ti,eff} = (1 - \varepsilon_{t,p}) c_{ti} + \varepsilon_{t,p} c_b$ $k_{ti,eff} = (1 - \varepsilon_{t,p}) k_{ti} + \varepsilon_{t,p} k_b$ <p>where</p> <p><math>v</math> – direction of the flow, which is volumetric flow of the unit area, <math>k_p</math> – perfusion conductivity; <math>t,p</math> – subscripts to indicate tissue porosity</p>	Discrete-vessel model describes the heat exchange between single blood vessel and surrounding tissue
Weinbaum, Jiji, Lemons, 1984-1992 [62 - 69]	$\rho_b c_b \pi r^2 \underline{v} \frac{dT_{art}}{ds} = -q_{art}$ $\rho_b c_b \pi r^2 \underline{v} \frac{dT_v}{ds} = -q_v$ $\rho_{ti} c_{ti} \frac{\partial T_{ti}}{\partial t} = \nabla k_{ti} \Delta T_{ti} + \left[ n q \rho_b c_b (T_{art} - T_v) - \rho_b c_b n \pi r^2 \underline{v} \frac{d(T_{art} - T_v)}{ds} \right] + q_m$ <p>where <math>q_{art}</math> - heat loss from an artery due to heat conduction through its wall; <math>q_v</math> - heat influx into a vein due to heat conduction through its wall; <math>T_{art}</math> and <math>T_v</math> - volumetric mean temperatures inside the blood vessel; <math>r</math> – radius of the vessel; <math>\underline{v}</math> – the speed of the flow through the artery or vein; <math>n</math> – number of the arteries and veins; <math>q</math> – blood flow velocity per unit surface area of the vessel.</p> <p>Or the simplified version of the Weinbaum, Jiji and Lemons model can also be used:</p> $\rho_{ti} c_{ti} \frac{\partial T_{ti}}{\partial t} = \nabla k_{eff} \nabla T_{ti} + q_m$ <p>where <math>k_{eff}</math> – effective conductivity, which can be defined as:</p> $k_{eff} = k_{ti} [1 + Pe_i V(\xi)],$ <p>where <math>\xi</math> – dimensionless distance, defined as <math>x/L</math>; <math>L</math> – tissue layer thickness; <math>V(\xi)</math> - dimensionless function of vascular geometry that can be calculated if vascular information is known; <math>Pe_i</math> – Peclet number, which is defined as:</p>	<p>The first two equations represent heat transfer in the main (in terms of the thermally significant) arteries and veins.</p> <p>The third equation describes heat transfer in the tissue that surrounds the couple artery-vein. The fourth equation is a simplified representation of the first three equations to estimate temperature distribution in the tissue</p>

$$Pe_i = \frac{2\rho_b c_b r_i v_i}{k_b}$$

where  $r$  – radius of vessel;  $v_i$  – blood velocity at the entrance to the tissue.

The biothermal mathematical equations presented in Table 2 can be described in terms of two main approaches: continuum and discrete-vessel models. The continuum model is the simplified type of biothermal equations, which describe the effects of the blood flow on the temperature distribution by considering the average blood supply over the average volume in the area of interest. The continuum approach was used in the works of Pennes [50] and Wulff's energy conservation equation [61].

The discrete-vessel model is a more advanced and sophisticated approach, which is based on biothermal equations describing the blood flow in each individual vessel in the area of interest. This approach was described in the works of Mitchell and Myers [36], Keller and Seiler [39], Chen and Holmes [40], as well as Weinbaum-Jiji-Lemons, which included a simplified version of their model [62-69].

Commonly used idealized mathematical models of Pennes and Wulf neglect such effects as heat transfer between blood and tissue, the blood flow, as well as the size of the blood vessels and their location relative to each other. Pennes' equation has a reasonable agreement with the experimental data and is often used to describe temperature distribution in the area of interest. The more sophisticated discrete-vessel model takes into account detailed information about the network vessel and blood perfusion. The approach takes into consideration the existence of temperature difference between arteries and veins, which are close to each other, and the heat transfer that occurs in opposite flow between them. The approach requires a set of biothermal equations describing the movement of blood in each individual blood vessel. Countercurrent flow is also considered and this has a significant impact on the heat transfer equilibrium. As a result, the temperature distributions can be predicted with higher resolutions in the adjacent tissues of interest. In particular, the mathematical model of Weinbaum-Jiji-Lemons can describe the heat transfer in the acentric tissues, where its assumptions are valid. Anatomy and vessel geometry data is needed in the application of the model. The data includes the density of the vessel, the size and distance between artery and vein, as well as blood perfusion rate.

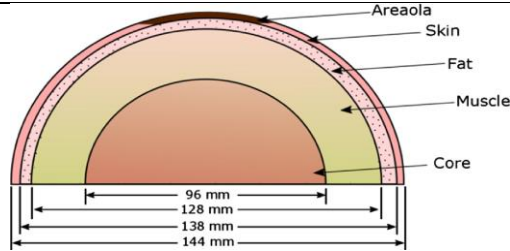
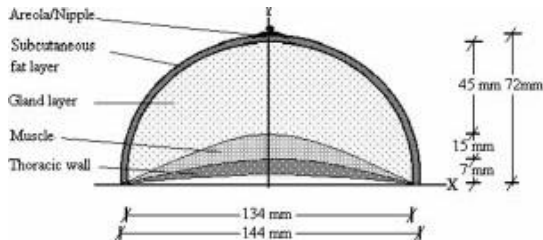
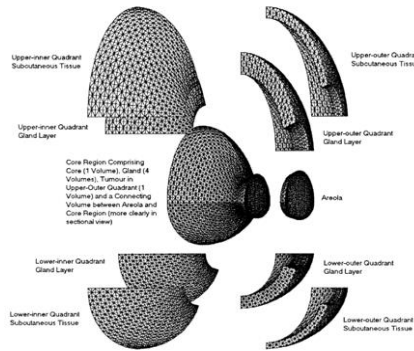
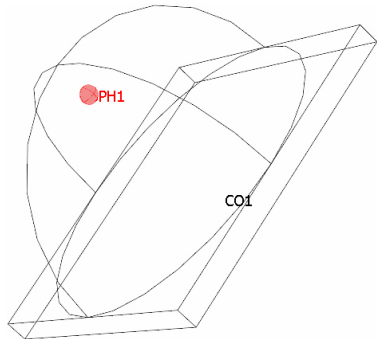
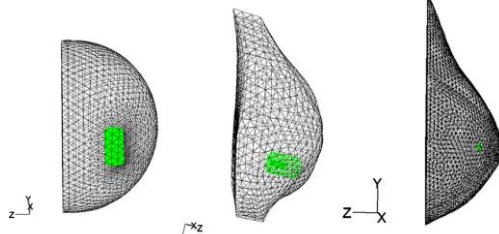
Many researchers used these mathematical models to study the effect of the blood flow and diameter of blood vessels on the temperature distributions. According to Chato et al. [41] higher blood flow decreases upon downsizing of the blood vessel, and therefore the heat transfer coefficient can be determined in countercurrent flow. Charny and Levin [70] studied the heat transfer between the artery and vein, and showed that thermal equilibrium of the system can be reached at the distance of 43 mm from the main vessels. In addition, it was established that the countercurrent flow can reduce the temperature of the tissue by 0.5 °C. These works illustrated the applicability of mathematical models. The choice of appropriate biothermal model should be based on the objectives of the study and specific biophysics features of the cases.

### 3.2 Breast geometry involved in simulations

The geometry of the breast is another important factor in the numerical simulations. Many different computational geometries were used in the thermal simulations and these included rectangular, idealized spherical, and realistic geometries of the breast [35, 71, 72, 73]. Table 3 presents the list of domains found in the literature.

Table 3. Computational domains

Study	Breast Geometry	Description
Osman, Afify, 1984; Osman,		2D and 3D models were developed to estimate the

1 2 3 4 5 6 7 8 9 10 11 12 13 14 15 16 17 18 19 20 21	<p>Afify, 1988 [74, 75]</p>	 <p>2D model of the breast [74, 75]</p>	<p>influence of the tumor size and location on the temperature distributions on the surface of the breast</p>
22 23 24 25 26 27 28 29 30 31 32 33 34 35	<p>Ng, Sudharsan, 2000 [76]</p>	 <p>2D breast model [76]</p>	<p>2D breast model was developed to perform analysis of variance, and parametric design by Taguchi method</p>
36 37 38 39 40 41 42 43 44 45 46 47 48 49 50 51	<p>Ng, Sudharsan, 2001 [77]</p>	 <p>3D breast model [77]</p>	<p>Flexible, multilayer finite element model was divided into four quadrants. The model was used to study steady state and time dependent numerical simulations</p>
52 53 54 55 56 57 58 59 60 61 62 63 64 65	<p>Gonzalez, 2007 [78]</p>	 <p>Ideal hemispherical model of the breast consisted of: hemisphere, chest wall, tumors [78]</p>	<p>Perfect hemisphere breast model used to study the required sensitivity of the thermal camera in order to identify tumour in the breast at the defined depth</p>
	<p>Bezerra et al., 2012 [79]</p>	 <p>Thermogram based 3D breast models [79]</p>	<p>The breast model was obtained manually and approximately based on simplified thermogram side view profiles and used to estimate the thermal conductivity and blood perfusion of breast tissues</p>
	<p>Das and Mishra, 2013 [80]</p>		<p>The study focused on the evaluation of predictive</p>

	<p>A 2D rectangular domain of the breast with width <math>2L</math> and height <math>L</math>. The domain is divided into three regions: Isothermal (bottom-left), Convective (top-right), and Adiabatic (right). A central square represents the tumor. Boundary conditions are: Symmetric at <math>x=0</math> (<math>\frac{\partial T}{\partial x} = 0</math>), Isothermal at <math>y=0</math> (<math>T _{y=0} = T_a</math>), Convective at <math>y=L</math> (<math>-k \frac{\partial T}{\partial y} = h(T - T_f)</math>), and Adiabatic at <math>x=L</math> (<math>\frac{\partial T}{\partial x} = 0</math>). The origin <math>(0,0)</math> is at the bottom-left corner.</p> <p>2D rectangular domain of the breast [80]</p>	<p>algorithms, where temperature distribution on the surface of breast was employed to study tumor behavior. Study used in-house numerical code and Pennes' mathematical model</p>
Das, Mishra, 2015 [81]	<p>An idealized 3D breast model represented as a sphere. A red wireframe sphere inside represents the tumor. Arrows indicate the radial location and angular coordinates of the tumor.</p> <p>Idealized 3D breast model [81]</p>	<p>The breast model used four parameters to define the tumor: size, radial location and two coordinates of two angular locations</p>
Amri et al., 2016 [82]	<p>A 3D rectangular breast model with dimensions <math>L</math> (width), <math>L</math> (depth), and <math>H</math> (height). The model is divided into three layers: Fat (top), Gland (middle), and Tumour (bottom). A spherical tumor is located within the Gland layer.</p> <p>3D rectangular breast model with a spherical tumour inside [82]</p>	<p>The study conducted steady-state and transient numerical simulations with cold stress to learn the influence of the depth on the temperature with Pennes' bioheat equation; a simple 3D rectangular breast model was used</p>
Hossain, Mohammadi, 2016; Saniei, et al., 2016 [83, 84]	<p>A multilayer breast model diagram labeled 'a)'. It shows a cross-section of a breast with layers: Skin (outermost), Fat, Lobule (innermost), and Muscle (bottom). A green lobule is shown within the fat layer.</p>	<p>Multilayer breast model was employed in the idealized hemisphere model and deformed hemisphere breast model. The model was used to estimate physio-thermo-biological parameters, such as depth, size and metabolic rate of the tumour</p>

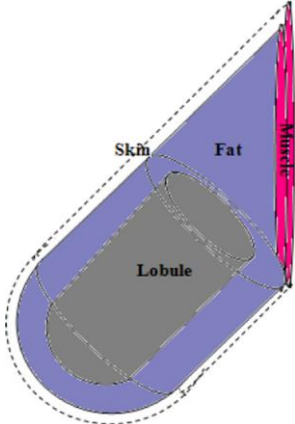
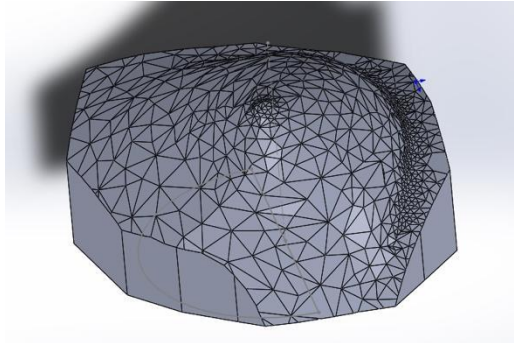
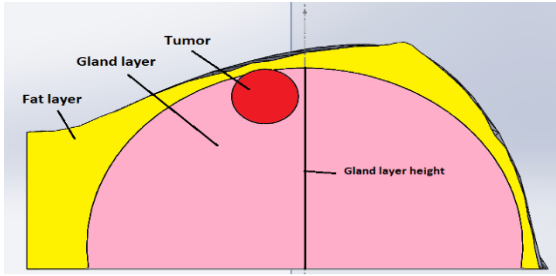
	 <p>b)</p> <p>Breast model: a) hemisphere breast model, four concentric tissue layers; b) deformed hemisphere breast model, four concentric tissue layers [83]</p>	
Mukhmetov et al., 2018 [73]	 <p>Patient's specific breast model [73]</p>	Patient specific breast model created by 3D scanning and used to estimate the temperature distribution based on the size and depth of the tumour inside the breast. Reverse thermal modeling was also conducted to obtain patients' specific tissue properties and tumour sizes and locations
Aitbek et al., 2019 [85]	 <p>Multilayer breast model [85]</p>	Multilayer breast model was used to estimate the influence of the density of the breast on the detection of the tumor

Table 3 lists the studies that used different breast geometries and predictive models to relate the temperature distributions to the tumor sizes, locations, metabolic heat generation and blood perfusion rates. Four main types of the breast geometries were developed in these studies [74-85]: rectangular, hemispherical, deformed hemisphere and patient-specific.

Osman and Afify [74, 75] developed a 2D multilayer breast geometry in 1984. The work was extended in 1988 using a 3D breast geometry to estimate the influence of the size and location of the tumor on the temperature distribution of the breast surface. This model was not used by other researchers as it creates high temperature differences in the layers close to the surface [86].

Further studies by Ng and Sudharsan [76, 77] led to improvement in both 2D and 3D multilayer breast models. They made 3D flexible models with tissue layers of different thicknesses and separated the geometry into four quadrants to investigate the temperature differences in the upper-outer, lower-outer, as upper-inner, and lower-inner segments. This model was widely adopted in many studies in the determination of the effects of different tumour parameters on the thermal distributions.

Gonzalez [78] used a hemisphere breast model and added a thick layer of 1.3 cm to simulate the chest wall. The results of the study revealed that Finite Element Simulations are able to detect 3 cm tumors located at the depth of 7 cm from the surface. Bezerra et al [79] modelled the breast geometry based on the silicone prostheses. The cylindrical geometry was improved with nodule type, size, depth and location extracted from an ultrasound examination of a patient. The study established the methodology to define the thermophysical properties of the breast tissues and nodules using maximum temperature from the temperature profile. Das and Mishra [80] in 2013 used a rectangular domain, single layer breast model with the Pennes' bioheat equation to diagnose a tumor based on the temperature distribution on the surface of the breast. The rectangular model does not reflect the real shape of the breast and it was difficult to validate the results with thermograms. As a result, no concrete conclusion was drawn. The authors later created a single layer 3D hemispherical model with a tumor [81], and found that the developed tool could be used not only to detect small tumors closed to the surface of the breast, but also big tumors located deep inside the breast, when there is a clear temperature difference on the surface of the breast. Amri et al. [82] used a 3D rectangular breast model to conduct steady-state and transient numerical simulations. Their results showed that the rewarming process after applying the cold stress gave more information about the tumor. However, the main problem with the rectangular breast models is that it did not correlate to the real breast geometry and its tissue layers. In addition, such breast geometry employed uniform properties for the tissue and tumour, which could not be validated by experiments.

There are many studies based on the rectangular and spherical computational domains, but very little technical literature on the use of personalized patients' breast geometries in numerical investigations. Mukhmetov et al. [73] created 3D numerical models by scanning a mannequin and real patients' breasts. The obtained numerical findings were validated by experiments using artificial and human breasts. Aitbek et al. [85] enhanced patients' specific model by creating different layers inside the breast and estimated the influence of the fat on the temperature distribution on the surface of the breast and thereby identify the tumor inside the breast.

### 3.3 Forward/direct and inverse simulations for breast cancer detection

Numerical modeling of the tumour inside the breast is a complicated process, however, it is a reliable technique to supplement thermography with quantitative assessments. The studies in which physical models are used to predict breast surface and volumetric temperature distributions are called forward or direct numerical simulations.

In the process of numerical simulation, the creation of relevant breast geometry is first required (see section 3.2) with proper boundary conditions. This is followed by numerically solving the governing mathematical equations (see section 3.1) in the breast domain. Researchers employed different approaches to solve Pennes' equation. Huang et al. [87] solved the Pennes' bioheat equation analytically for two cases, which differed in terms of arterial temperature. In the first case arterial temperature was equivalent to the mean temperature of the vessel while in the second case the arterial temperature was constant. Zhang [88] solved the bioheat equation using the Lattice Boltzmann Method, which generated precise temperature distribution. Okajima et al. [89] solved the one-dimensional Pennes' bioheat equation and derived two general bioheat transfer dimensionless characteristics for steady-state condition.

Many studies solved the bioheat equation in different coordinate systems. Gupta et al. [90] solved the bioheat equation in spherical symmetric, axisymmetric and Cartesian coordinate systems by using the Galerkin's method. By solving the heat equations in different coordinate systems and considering different breast models, researchers revealed that the location and size of the tumour inside the breast have primary effects on the temperature distribution on the breast surface.

Such studies as in [7, 9, 54, 74 - 77, 82, 86, 88, 91] concluded that the temperature patterns depended on the diameter and depth of the tumor, and agreed that small and deep seated tumours were difficult to detect, as the temperature patterns had low contrast in the surface temperature distributions. Das and Mishra [80] studied the influence of depth on the patterns of the temperature distributions, by calculating the temperature differences between 12.5 mm and 37.5 mm diameter tumours at the depth of 12.5 mm. Their



results showed the differences of surface temperature of 0.007 °C and 0.56 °C, respectively. Amri et al. [82, 91] determined the temperature differences for different sizes of the tumors from 10 to 30 mm at the same depth of 20 mm. The results showed the temperature differences of about 0.2 °C for tumours of 10 mm and 30 mm (Figure 1), which revealed that the size of the tumour does not have much influence at the depth of 20 mm and deeper. Ng and Sudharsan [76, 77] reported that tumors deeper than 38 mm have a very low chance to be detected by IR camera. These results confirmed that the depth of the tumour has significantly more influence compared with the tumour diameter. The depths at which the tumours most probably cannot be detected ranged from 20 mm to 30 mm.

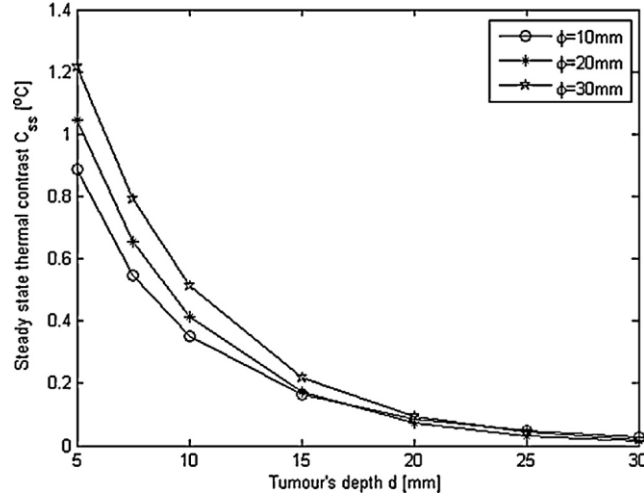


Figure 1. Steady state thermal contrast as a function of tumour diameter and depth [82]

The temperature contrast on the surface of the breast can be increased by applying cold stress. This phenomenon was elaborately described by Usuki et al. in [47]. The cold stress can enhance the temperature difference between the healthy tissues and those afflicted by cancer, and thereby improve the detection of breast cancer. In order to estimate at what rate the thermal contrast can be enhanced the penetration depth of the cold stress is calculated. The penetration depth ( $\delta$ ) is determined as the length in the direction normal to surface at which the temperature equals to  $0.99T_i$  and can be defined as a function of thermal diffusivity ( $\alpha$ ) and time ( $t$ ) [92]:

$$\delta = 3.65\sqrt{\alpha t} \quad (1)$$

Thermal diffusivity is determined by the equation of transient conduction equation in one dimension [92]:

$$\frac{\partial^2 T(x,t)}{\partial x^2} = \frac{1}{\alpha} \frac{\partial T(x,t)}{\partial t} \quad (2)$$

where  $T$  is the temperature,  $x$  is length in the direction normal to surface,  $t$  is the time;  $\alpha$  is the thermal diffusivity. At the condition when:  $T(x=0; t>0) = T_o$ ;  $T(x \rightarrow \infty; t>0) = T_i$ ;  $T(x>0, t=0) = T_i$ , where  $T_o$  is the temperature of the cold stress;  $T_i$  is the temperature of the tissue.

According to Gonzalez-Hernandez et al. [92], the thermal diffusivity of the glandular tissue is equal to  $1.52 \times 10^{-7} \text{ m}^2/\text{s}$  (Figure 2b). Therefore, for the tumours at a depth less than 20 mm, the time of applying cold stress equals to about 4 minutes, whereas for the tumours at the depth of more than 30 mm this time is more than 9 minutes.

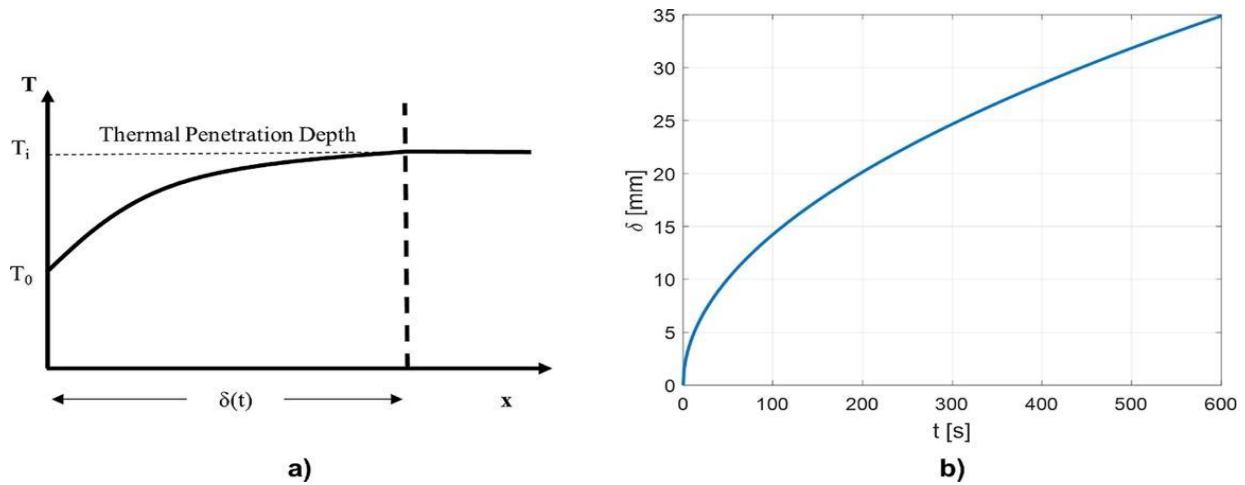


Figure 2. Penetration depth: (a) schematic representation; (b) function of time [92]

According to the study of Chanmugam et al. [93] the penetration depth varied with the time of applying the cold stress. For the duration time of 2 minutes the penetration depth equaled 6 mm, measured at the points along the axis, considering a decrease of the temperature of  $0.3^\circ\text{C}$ , as matched to the temperature under the same conditions in steady state. The authors established that the mostly observed temperature difference between the healthy and cancerous tissues was between 10 to 20 minutes after the cold stress was applied. Furthermore, the research of Amri et al. [82] revealed that for the same depth of 20 mm the estimated time for the cold stress was 2 minutes at the cooling temperature of  $15^\circ\text{C}$ . Such time of cooling is enough to achieve the maximum thermal contrast. However, this cooling time is not enough for the tumors deeper than 20 mm, as longer observation and cooling time is required.

By contrast, Ng and Sudharsan [77] analyzed the effect of cold stress on the temperature distribution, as well as the rewarming process. The study made numerical calculations for the cases of 1, 3 and 5 minutes of applying the cold stress. The results of the study showed a temperature increase between 0.05 and 0.045 in non-dimensional terms; such a thermal contrast did not give any valuable information on the temperature pattern. The authors revealed a thermal contrast of  $0.16^\circ\text{C}$  during the observation of the rewarming process of 60 minutes, and based on the study of Usuki et al. [47] concluded that such thermal contrast was enough to clearly detect the abnormality. Moreover, another study of Jiang et al. [54] concluded that in order to achieve the required thermal contrast the minimum cooling time should be 25 minutes at the cooling temperature below  $15^\circ\text{C}$ , which was not possible because of the highly uncomfortable condition for the patients. Thus, transient numerical simulation was conducted to find ways of increasing the thermal contrast of the healthy and cancerous tissues.

However, the results of most of these studies were impractical. The reason is either the simulated breast domains did not represent the real ones, or the structures of the numerical breasts did not reflect the actual ones. Furthermore, the boundary conditions of the studies also did not coincide with the real conditions. In this regard, it is better to simulate convection around the breast because of the cooling of the breast, and thereby to achieve higher accuracy in tumour detection.

Detecting abnormality in thermograms is not only for diagnosis, but also for extracting detailed patient specific information of the tumour, such as the size, depth, heat generation or blood perfusion, which can be performed as an inverse problem. This is a different type of problem, especially when one considers that for one thermogram there can be various combinations of tumor sizes and locations [74, 75].

Inverse modeling is the evaluation of the indefinite model parameters when the solution is identified (Figure 3). For breast cancer detection using thermography, the obtained surface thermogram is one of the solutions for the bioheat equation. In order to perform inverse thermal modelling, there are several steps to follow: 1) create a computational breast domain (section 3.2); 2) set the boundary conditions for the selected bio-heat equation; 3) apply one of the optimization tools to search for the right parameters; 4) solve the bioheat equation and evaluate newly obtained solution; 5) repeat the steps 3) and 4) until the appropriate



parameters are found. The aim of the inverse modelling is to search for the right parameters so that the solution matches the input surface temperature distribution provided by the thermogram. The most frequently used tools for the optimization are: Levenberg-Marguardt algorithm, Genetic Algorithm and Gradient Descent Method.

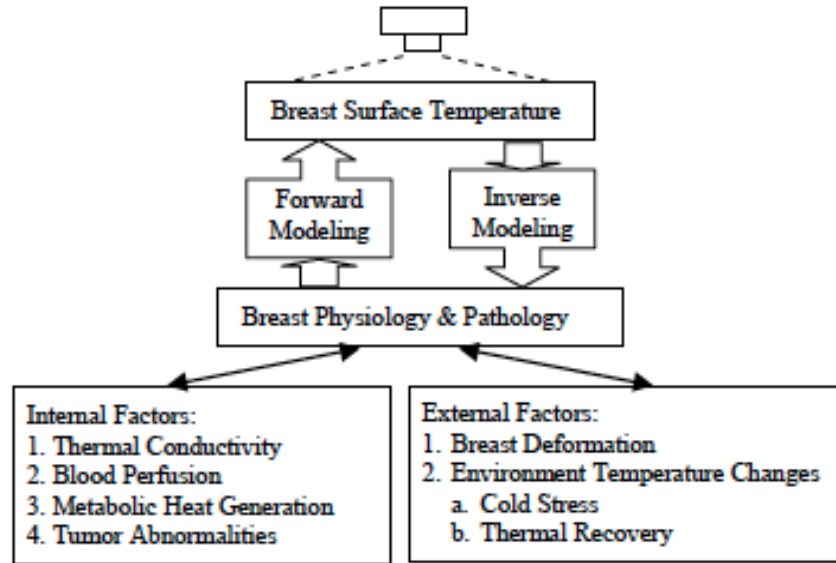
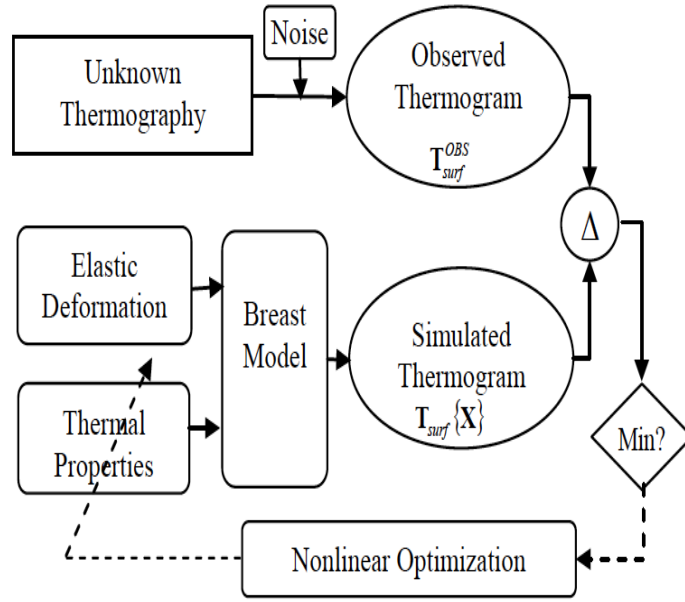
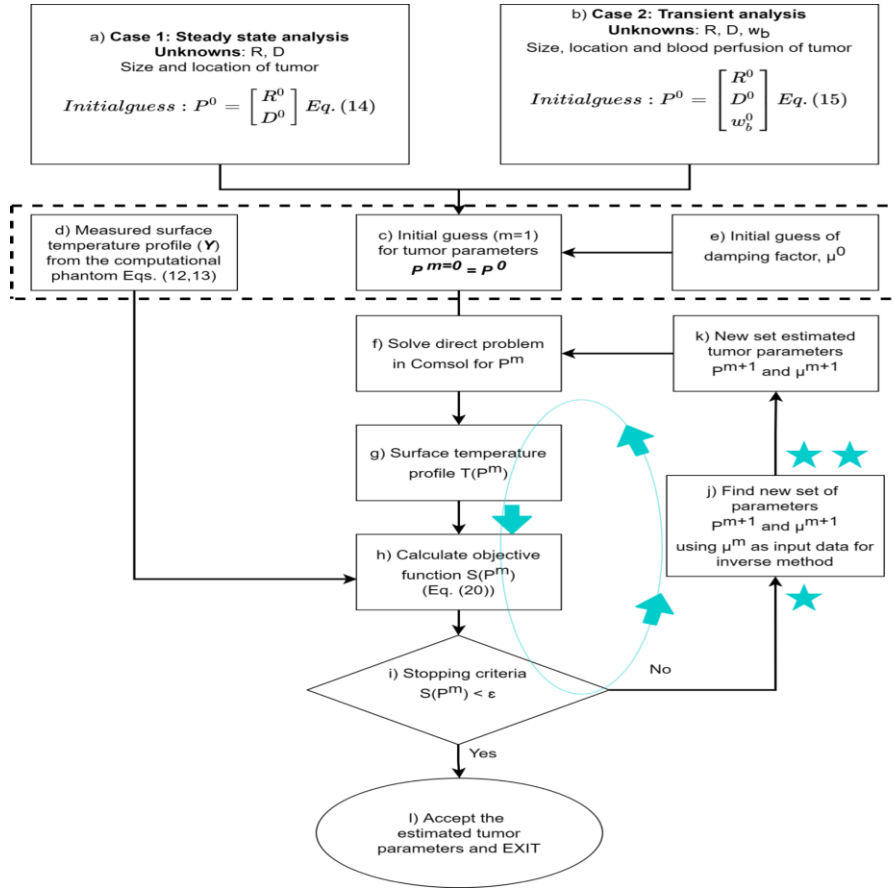


Figure 3. Diagram of thermal direct/forward and inverse modeling [94]

The Levenberg-Marguardt (LM) algorithm was used in two studies conducted by Jiang et al. [94] and Hatwar and Herman [95]. Jiang et al. [94] employed the LM algorithm using the primary thermal parameters and developed an inverse method of evaluating thermal parameters of the tissues based on the temperature distribution on the surface of the breast. In order to evaluate the normalized thermal parameters the authors explored the iterative nonlinear optimization (Figure 4a). The results of the inverse modeling for the tumors' sizes of 8 and 16 mm showed improvement in the detectability of the tumors regardless of the tumor depth. The tumor-detection correlation coefficient had values almost equals to 1. Hatwar and Herman [95] implemented the scheme shown in Figure 4b. The authors argued that steady state data were not enough to simultaneously estimate three parameters (location, size and blood perfusion). Therefore, the authors included into the study transient modelling in order to accurately estimate locations and sizes of the tumors, and then attempted to include evaluation of blood perfusion as well. For the inverse reconstruction the authors employed an LM algorithm (Figure 4b) using the temperature distribution on the skin surface to characterize the tumor. The study used tumor parameters with the following ranges: 12 mm to 30 mm in depth, 7 mm to 11 mm in radii and blood perfusion rate ranging from 0.003 1/s to 0.01 1/s. The results showed that the accuracy of detection decreased as the depth of the tumours increased. The tumours with 0.01 1/s in blood perfusion rate and 11 mm radii showed high accuracy if they are at the depth of 20 mm from the surface of the body. Thus, the method showed its consistency, while it can still be further improved by employing computer tomography (CT) images and improving the accuracy of the blood perfusion for large tumours.



a)



b)

Figure 4. Flowchart showing inverse reconstruction algorithm for the studies: a) [94]; b) [95]

There are several studies that employed Genetic Algorithm (GA) and Artificial Neural Network (ANN) or curve fitting method to evaluate the size, location and metabolic heat generation of the tumour. Mital and Pidaparti [96] used ANN first to map the obtained thermograms, and then employed GA to search the tumour parameters such as size, location and metabolic heat generation rate (Figure 5a). The study



obtained results and to develop sustainable procedures. Therefore, thermography can be further improved by developing intelligent thermogram-based systems using more patient-specific data/information, artificial intelligence and machine learning techniques.

#### **4. From computer-aided diagnosis (CAD) system towards intelligent thermogram-based CAD systems**

##### **4.1 Computer-aided thermogram-based diagnostic system**

There are many studies conducted to improve IR imaging as a prognostic, adjunct, breast cancer earlier detection tool, and the trend for future research seems to be in the area of computer aided diagnosis (CAD). A CAD system includes such components as: digital image processing, artificial intelligence, personalized data and physical modelling, and machine recognition of temperature distribution patterns. The main advantages of the CAD systems are: 1) it is less dependent on the human subjective opinion; 2) it is a quantitatively based system, which can reduce false positive or false negative results; 3) it reduces expenses of any additional medical procedures; 4) the system could be automated.

Development of thermography into a complete CAD system involves many stages [45, 103, 104, 105]: 1) image capturing and eliminating noises without losing vital details; 2) segmentation of the region of interest (ROI); 3) selection and extraction of thermogram features; 4) organization of selected features into databases; 5) characterization and classification of tumors into the probability of malignancy and any abnormalities; 6) data mining by using machine learning technologies (MLT) [106, 107], including K-nearest neighbors (K-NN) [108], Artificial Neural Network (ANN) [109, 110], Decision Tree (DT) [111, 112], Support Vector Machine (SVM) [113, 114] and Bayesian Networks [139-146].

The most important development in an intelligent CAD system is the segmentation of ROI and then its selection and extraction. Therefore, a number of studies are dedicated to improve the approach to understand and differentiate features of healthy and tumorous breasts. One of the first studies, which focused on facilitating the comparison process, was the study by Lipari and Head [115], who segmented the thermograms into different quadrants so that the differences in temperature between the contralateral breasts could be more visible. To eliminate diagnosis errors due to human interpretation, the work was extended to include the automated comparison of the temperature profiles on contralateral breasts [116]. Their findings indicated that the system accuracy can be improved by comparing the statistical analysis of entire breasts with those obtained from different quadrants. Another work done by Qi and Head [117] and Kuruganti and Qi [118] also studied the way to automatically select and extract special features of the healthy and diseased breasts from thermograms. The authors suggested implementing it through pixel distributions in accordance with different quadrants in which two breasts were divided.

While some studies aimed to improve the image processing and segmentation, the other studies tried to exclude the influence of human errors from the diagnosing process. One of such studies, conducted by Irvine [119] explored automated target recognition as a tool that could be employed in order to avoid human errors in the diagnosing of the breast tumor. Further work by Jakubowska et al. [120] and Wang et al. [121] developed an automated system for comparing thermal images, where the main purpose was to understand the differences in thermal characteristics between breasts with and without malignant tumors. In the area of segmentation there is one more work done by Schaefer [122], who used statistical tools together with a fuzzy rule-based classification system for the diagnosis of patients, and the study achieved an accuracy of 80%. In [123] the authors explored the horizontal projection and vertical projection profiles in order to segment two breasts. The possibility of using a structured approach for detection of abnormal changes in the breast based on thermography was investigated by Morais et al. [124]. The method utilized conjugate gradients to compare the measured dimensionless temperature differences between two symmetric regions of a subject's breasts, taking into consideration the human body bilateral symmetry and ambient conditions. The methodology was able to detect 96% of breast lesions. The results demonstrated that the thermography-based system has an opportunity to be used as a simple, cheap, noninvasive mass screening tool for early breast cancer detection. Further studies in the area of breast cancer detection using thermography were also aimed to facilitate the process of feature extraction and classification. In this regard the work done by

Pramanik et al. [10] can be highlighted, as the authors came up with a feature extraction technique, that allowed to capture the edges and valleys of the thermal breast images for texture analysis, and then to classify them by exploring feed-forward artificial neural network. The rate of true positive recognition was equal to 100% and false positive outcome was 0. Another study, which developed the methodology of automatic segmentation of the breast image was proposed by Garduno-Roman et al. in [11]. The authors used Otsu's method for automatic thermogram segmentation and also explored watershed approaches to differentiate abnormal regions of the breasts. The methodology was validated based on the database of Mastology Research and 454 cases were tested according to the developed methodology. The established methodology showed the sensitivity and specificity equaled to 0.8684 and 0.8943, accordingly, and 90.3% of segmentation accuracy. The authors of the studies mentioned above agreed that thermography with the combination of automated CAD systems can be used as a supportive and adjunctive tool for earlier breast cancer detection.

Although some developments have been achieved for CAD systems based on IR thermography, there are many areas that still need to be improved. These areas include: 1) automation of the CAD systems [115, 122, 123]; 2) representation and processing of thermal images. This is vital for further improvement of the efficiency of the CAD systems. Currently, thermal images and breast geometries are separately represented in different formats. As such correlation between 2D thermal characteristics and 3D breast properties can be limited. This area has room for exploration and improvement; 3) feature extraction and classification methodologies. These are the core to support automatic prognosis. With effective features, undesirable regions can be identified and automatically removed. Features would also assist classification and pave the way for the creation of repository and intelligent diagnosis. This is a critical area for the development of the CAD systems.

Moreover, it is envisaged that the role of thermography-based CAD systems is to complement, but not to replace mammography. Therefore, according to the conducted research thermography-based CAD systems can identify suspicious cases; therefore, such cases might be further referred to more detailed mammography and biopsy examinations. In addition, as thermography is noninvasive more frequent measurements can be made, as a result more accurate diagnosis can be achieved through the process of continuous temperature measurements of the breast. With modern Internet facilities and the advancement of 5G Internet facilities, the data can be instantly updated to ensure timely intervention, and thus thermography-based tele-CAD systems have great potential to facilitate mass breast cancer monitoring in remote areas where medical equipment may be lacking.

#### **4.2 Application of Artificial Neural Networks (ANNs) in breast cancer detection**

Early detection of breast cancer by IR imaging can be improved through integrating the tool with other approaches. Artificial Intelligence (AI) is considered as a group of algorithms that can study features from data and most AI algorithms used for the detection of breast cancer are mainly related to classification. The objective of such algorithms is to separate healthy breasts from those with malignant tumors. They need to be trained with thermographic images for both healthy and malignant breasts [1]. The most useful application of AI is Machine Learning (ML), which focuses on pattern recognition and computational learning theory of AI. The ML can be used to construct algorithms that might learn from data and create relationships with computational statistics and mathematics. There are many ML algorithms such as Naïve Bayes, Support Vector Machine (SVM), Decision Tree (DT), Relevance Vector Machine (RVM) and Artificial Neural Network (ANN).

Artificial Neural Network (ANN) is a widely used analytical tool, which assists physicians in diagnosis of patients with breast tumors. ANN represents a bio-physiological model of the human brain attempting the imitation of its operations. The ANN's important building block is processing elements, which are combined by the ANN in various architectures in order to achieve a range of computational capabilities [1]. Numerous images both with and without breast cancer are provided for ANN to feed the input layer and to be processed in the hidden layers. The output of the hidden layers functions as input to the neurons in the output layer that subsequently leads to decision making. Due to the capability of the



ANN in providing fast evaluation and precise results this tool is more preferable in comparison with other classifiers [125].

Ng and Kee [71] used both ANN and bio-statistical approaches to diagnose cancerous tumors from IR thermograms. They analyzed thermograms of 82 patients (including 30 asymptomatic, 48 benign and 4 malignant) and identified the inputs of the ANN by the use of a regression analysis. According to the authors' report the maximum accuracy in detecting the tumor was 80.95%, while the accuracy of the radial basis function neural network in making a true diagnosis was 75% in the unhealthy population, and 90% in healthy population.

Mital and Pidarati [96], combined the ANN, GA, and thermal simulations to connect the temperature of the skin surface with the depth and diameter of the tumour. To predict the distribution of surface temperature, they trained the ANN with the tumor characteristics. Then the obtained surface temperatures were applied to the GA to find the appropriate parameters of tumor based on a layered semi-spherical breast. The errors of the tumor's depth and diameter identified by the GA and ANN were within 5 mm and 2 mm respectively.

The study in [1] established a framework for the incorporation of the ANN with thermography, four ANNs were developed and studied based on hospital data. Based on the study's findings, it was concluded that the achievement of better-trained neural networks and more accurate detection process as well as reduction of contradicting inputs are impossible without a large population. The application of breast thermal samples generated by thermography and numerical simulations as inputs is another possible approach to train the ANN. It may give a better-trained network as the ANN is a good pattern recognizer. A poorly trained network gives inaccurate results, thus using numerical inputs can greatly improve the training, since changing tumor parameters in a numerical breast model produces new training data and the number of available cases becomes unlimited by the amount of clinical data. This is considered as the benefit of using computer simulations in the ANN training. At the same time, in order to produce precise surface temperatures the numerical model must be well validated by clinical data. Finally, a well trained ANN can be employed as an initial screening tool to process thermograms before the numerical thermal inverse modeling is used for actual diagnosis of tumours.

Saniei [84] suggested a method that can be used to estimate tumor depth, size and metabolic heat generation rate. A dynamic neural network and surface temperature distribution retrieved from breast thermal images were used to assist the inverse thermal modeling. In order to confirm the approach, a number of cases with various tumor depths and sizes were explored. For the first step, a finite element thermal model was constructed and simulations were carried out. Similar thermal models were used as the bases for the inverse modeling step, where surface temperatures were employed as inputs to the models in order to search for the tumor parameters (depths and sizes). Results of the research demonstrated that the estimated error of depth was higher than the estimated error of size. The deep-seated tumors also had larger errors than other cases. The findings matched actual parameters and offered the possibility of determination of necessary parameters from a group of surface temperature data.

Wahab et al [126] suggested the improvement of the ANN for tumor localization by the use of thermal data gained from the prior works. They employed multiple features retrieved from a range of numerical simulations carried out by the use of different tissue compositions of breast models which were fed into the optimized ANN system of 6-8-1 network architecture with a momentum constant value of 0.3, iteration rate of 20000, and a learning rate of 0.2. The total accuracy of the results for testing and validation were 96.33% and 92.89% respectively. The larger error was probably obtained because of a large number of neurons chosen that were demonstrated previously to increase the training complexity.

The study of Pramanik et al [10] presented an automatic method of breast thermograms analysis. Their approach consists of three main steps including segmentation of breast regions from the original images, extraction of features, and classification and performance analysis by the use of ANN. The background area was removed in the segmentation phase through application of Otsu's thresholding approach followed by a reconstruction method. Lastly, the feed-forward ANN with gradient descent training rule was employed as a classifier. The main problem of the study was the limited collection of

breast thermal databases in open access. The authors explored 306 breast thermograms of 102 patients gathered from the Visual Lab [127]. The accuracy, sensitivity and specificity obtained in the proposed system were 90.48%, 87.6%, and 89.73%, respectively.

Thus, the reviewed articles show high accuracy of ANN used in combination with other approaches to diagnose the breast tumor. The results of the studies coincide with the actual parameters and thereby provide the opportunity to identify required parameters from a group of surface temperature data. Bringing together the ANN, GA, and computer simulations that connect breast surface temperature with tumor depth and diameter, and heat generation, in which the breast is considered as a domain of calculations, may offer further improvements in diagnosis. Therefore, ANN, GA and computer simulations can be further studied to establish an intelligent system for breast cancer detection.

Over the past few years, Physics Informed Neural Network (PINN) [128, 129] has emerged as a hot research topic for solving heat transfer and fluid flow problems as an arbitrary hybrid data-driven and physics-driven simulation method since it uses both the residuals of the underlying governing differential equations based on physics laws and input data in the loss function for NN (Neural Network) training. This means that PINN can use arbitrary amounts of data and use more physics in the machine learning (ML) processes, which helps to overcome the limitation of traditional ML techniques for finding solutions. For example, thermograms and 3D scans for the breast can be supplied to PINN as input data while the heat transfer equations in the breast and the Navier Stokes equations for the air flow outside the breast can be used to train the ANNs to predict heat transfer and fluid flow, as well as patient specific tissue properties and tumor sizes and location simultaneously. Thus it is expected that PINN may be the next generation analysis and diagnostic tool that combines the best of the physics-based and data-driven simulation.

#### 4.3 Application of different machine learning techniques for breast cancer diagnosis

One of the discriminative classifiers largely employed in breast cancer diagnostics is a Support Vector Machine (SVM). SVM is formally identified by a separating hyperplane. One of the earliest studies on the SVMs was carried out by Acharya et al. [130] who used them to classify 50 IR thermograms of breasts, including 25 breasts with a cancer tumor and 25 normal ones. Various statistical indicators such as the mean, homogeneity, energy and entropy of the thermograms, were extracted by the authors. The application of the SVM led to a specificity of 90.48% and a sensitivity of 85.71%. The sensitivity here is higher than the typical sensitivity of 78% achieved by an expert radiologist. Although the results gained by the authors were promising, the number of tests and size of database used by them for training were too small. Therefore, it is impossible to generalize these results.

Tan et al. [131] employed 5 different classifiers, including feed forward and probabilistic neural network, fuzzy classifier, Gaussian mixture model and the SVM. 6000 temperature sets were collected from 16 thermocouples placed on the patients' breasts (16 thermocouples per patient or 8 on each breast). For the research purpose, Tan et al. [132] used 5000 and 1000 data for training and testing the classifiers respectively. The specificities, which all classifiers reached, were above 80%. The SVM showed the best performance with an average accuracy of 90.4% [131].

Gayathri and Sumathi [133] employed a Relevance Vector Machine (RVM) to detect breast cancer by creating a user-friendly environment for its diagnosis. In their study the authors compared the RVM to SVM, and the first method showed better results than the second one. The research demonstrated the differences between the variables and their accuracies, which were not much because the accuracy was up to 96%.

The study of Gogoi et al. [134] aimed to assess the effectiveness of highly sensitive Infrared Breast Thermography (IBT) in early diagnosis of breast abnormality. Their study examined the effectiveness of the IBT by conducting Temperature-based analysis (TBA), Intensity based analysis (IBA), and Tumor Location Matching (TLM). To distinguish healthy, malignant and benign breast thermograms in the TBA and IBA from each thermogram a number of temperature and intensity characteristics were retrieved, from which then thirteen various sets of features were identified. Their classification performances were assessed through the SVM with Radial basis function kernel. Among all sets of features that one, which included

statistically significant ( $p < 0.05$ ) features, provided the maximum classification accuracy of 83.22% with 73.23% of specificity and 85.56% of sensitivity. Thus, according to the results of the study, the IBT was found capable of being applied as a proactive technique for detecting the early breast abnormality in asymptomatic population.

Bharathi and Anandakumar [135] adapted a machine learning method for cancer classification in order to identify a proper algorithm based on the precision of these methods. They used the lymphoma and leukemia dataset and the Analysis of Variance (ANOVA) model to select the features. Selected features were applied to machine learning algorithms such as Fast Support Vector Machine Learning (FSVML), Fast Extreme Machine Learning (FEML) and Relevance Vector Machine Learning (RVML), in which RVM demonstrated better accuracy of higher than 95%. Tcheimegni [136] adopted a Kernel-based RVM in order to classify cancer diseases. In this study the author developed a hierarchical Bayesian model using sigmoid kernel and Radial basis function (RBF). The author also attempted to classify various diseases on the basis of clinical data by using the data driven model. By comparing the RVM and SVM, the author determined that the RVM demonstrated better accuracy than SVM of higher than 90%.

Bharathi and Natarajan [137] conducted classification of cancer through SVM and RVM based on the ANOVA model. The core of their research was the selection of smallest genes from microarray data in order to classify cancer effectively. The ANOVA was applied for feature selection. The selection was made by a ranking scheme. The selected genes were introduced in the SVM and RVM, in which the RVM demonstrated higher accuracy of more than 93%.

Rana et al [138] conducted a comparative study in which they used different machine learning methods such as Support Vector Machine (SVM), Logistic regression, K-nearest Neighborhood (KNN) and Naïve Bayes for detecting breast cancer and anticipating its recurrence. The accuracy of results for diagnosis of breast cancer was 95.6% and for predicting the recurrence and non-recurrence of breast cancer was 68%.

Nguyen et al [139] developed a computer aided detecting system for classification of both benign and malignant tumors. They employed the Backward Elimination (BE) approach jointly with Random forest tree method for feature selection, which consisted of totally 33 variables and then was diminished to 17-18 variables. The accuracy of this hybridized algorithm is demonstrated to be near 99%.

Silva et al [140] conducted a study that proposed a hybrid methodology of supervised and unsupervised machine learning to examine dynamic infrared thermography for diagnosis for patients with breast cancer. The dynamic infrared thermography quantitatively measured or monitored the changes of temperature on the breast surface after thermal stress. Test results confirmed the diagnostic ability of proposed methodology for patients with breast cancer. It should be noted that the classification algorithms such as K-Star and Bayes Net, demonstrated 100% classification accuracy among 39 tested cases. Moreover, the accuracy obtained among such classification algorithms as Bayes Net, multilayer perceptron, decision table and random forest consisted of 95.38%. The proposed approach could detect patients with potential cancer independent of the location of disease in the breast, however, it did not allow to determine the position of the abnormality in the breast.

#### **4.4 Detection of breast cancer using thermographic data and Bayesian Networks**

Sometimes there is a misunderstanding and confusion about the value and wide applicability of Bayesian networks (BNs). One of the reasons for confusion is that BNs can be used for both unsupervised/supervised learning (and so they sound similar although they are very different to ANNs) and for decision making encapsulating utilities (decision theory). The fundamental potential of BNs is that they comprise a mathematically consistent knowledge representation framework. Therefore the nodes of the network are representing pieces of knowledge that make sense. Mathematically the probabilistic nodes are random variables. Thus, a trained BN can be understandable and readable and also can be used to teach someone. The same is not true for ANNs which are like black boxes. ANNs are better for some tasks like image recognition. In the case of thermography BNs can be used both for predicting the tumor but they can also be used to construct a holistic decision making tool that can drive the correct diagnosis based on



information from thermography via Bayes Net and/or via ANNs as well as utilizing other methods. Furthermore, a BN expert model can also encapsulate certain or uncertain knowledge, extra tests, other risk factors or physicians beliefs to make the final diagnosis after thermography.

*Bayesian Network Classifiers* assign class labels to unlabeled cases, the classification finds a function that associates each unlabeled case to its corresponding label (class). The Naive Bayes classifier (NB) is one successful and popular classifier. A benchmark with respect to it, other classifiers have to be tested. An NB achieves learning from training data samples. Learning in the case of BNs means to construct the conditional probability of each state of variable given the class. NB for a new case, applies Bayes' rule and after selects the value of the class with the highest posterior probability.

The authors in [141] proposed a diagnostic method based on a score formed from thermographic data. 16 variables had been used to calculate this score (they comprise the nodes of the BN). The diagnostic power of the proposed variables was also estimated. 98 cases (21 healthy) had been examined and were used to build a diagnostic model and calculate its accuracy, sensitivity, and specificity.

The authors have applied the BN method with three different types of classifiers and compared this method with other techniques such as ANNs and decision trees. They confirmed that the advantage of BNs was that they permit someone expert/physician visually to determine which factors have an influence over the diagnosis outcome and how variables influence each other. ANNs exhibit similar performance but they lack explanation. They cannot explain how a decision is made and which are the critical variables that influence the diagnosis more. Decision trees have a limited explanation capability, but they cannot encapsulate interactions of explanatory variables. The analysis in [141] reveals poor specificity but very high sensitivity and accuracy. Larger and more balanced thermographic dataset is required.

In [142] the authors studied again with BN networks and various classifiers with the same dataset in [141]. They reconfirmed the results of [141] regarding accuracy sensitivity and specificity. The main conclusion was that the thermographic variables were subjective and should be reconsidered. The analysis with the help of the Bayesian network showed that only 2 out of the 16 variables influenced the diagnosis. A more balanced and larger dataset is needed.

The authors in [141] suggested to use 20 statistical quantities as characteristic variables to extract information from thermographic images. These variables were texture features extracted from the Gray Level Co-occurrence Matrix (GLCM). This Matrix otherwise called gray level spatial dependence matrix evaluates the spatial relationship of pixels. The GLCM values the texture of the thermography image, estimating how frequent pairs of pixels with certain values and in a given orientation " $\theta$ " and distance " $d$ " from each other happen in an image. Thus, this paper answers to the subjectivity issues of the variables that have been chosen in papers [141, 142].

In [143] the classification of the healthy and unhealthy cases had been done using three different classifiers: Support Vector Machine (SVM), K-Nearest Neighbor classifier (k-NN) and Naive Bayes classifier. In this paper the sample is small 26 normal and 14 abnormal images were studied. ROC analysis showed that the best accuracy was achieved with k-NN classifier. In this work the accuracy achieved was high but the dataset needed to be enlarged for safer conclusions and diagnosis.

In [144] the authors proposed a hybrid methodology using unsupervised and supervised learning techniques. In the previous works [141-148] supervised learning was only utilized. Another difference of this work was that Dynamic Infrared Thermographic data was used. Therefore the datasets were time series. The IR camera monitored temperature gradients, after a thermal stress. The first step of their method was to perform a clustering by k-means algorithm. Next, classification using Bayesian networks, neural networks, decision rules and decision tree was carried out. In this work 40 healthy cases and 40 with cancer cases were considered. The analysis in [144] was quite thorough. The authors executed 39 different classification algorithms. K-Star and Bayes Net outperformed and resulted in 100% accuracy. One drawback of this method is that it cannot determine the location in the breast tumor. Reverse thermal engineering is required for such a task.

In the work in [145] a larger set of thermographic data had been used. 1052 images were analysed. Another improvement that this paper introduced was that the images were classified into malign, benign,

cyst and normal groups from specialists and biopsy. Thus, the training and the final diagnosis concerned 4 different states and not just two like in all other reviewed works of this subsection. A third improvement in [145] was that the authors defined as variables attributes based on both geometry and texture. They used the so-called Zernike geometry moment (projections of the image function in orthogonal basis functions) and Haralick texture moment (co-occurrence matrix of the image). The classifiers executed were Bayes Network, Naive Bayes, Support Vector Machines (SVM), Knowledge Tree J48, Multi-Layer Perceptron (MLP), Random Forest, Random Tree, and Extreme Learning Machines (ELM). The analysis resulted in a fair accuracy with ELM and MLP doing better. However, the Bayesian networks also provided very good accuracy and much better if the variables in use exhibit independence. It is obvious that in [146] the combination of all these features concerning geometry and texture include variables that are correlated.

Finally, in [147] the authors proposed a method to diagnose normal or abnormal images (with cancer or without). The novelty of this work is the use of the combination curvature function and gradient vector flow method for breast segmentation. Furthermore, in this work the classification analysis used the new powerful type of ANN called convolutional neural networks (CNN). The authors presented in [148] a comparison of CNN with tree random forest (TRF), multilayer perceptron (MLP), and Bayes network (BN). CNN technique outperformed the rest and succeeded with perfect accuracy. The dataset was not that large and had only 73 breast images, but the overall efficiency was very high and CNN was found to have 100% TPR (true positive rate or sensitivity:  $TPR = TP / (TP + FN)$ ), SPC (specificity or true negative rate:  $SPC = TN / (TN + FP)$ ), and ACC (accuracy:  $ACC = (TP + TN) / (TP + FP + TN + FN)$ ).

In summary Bayesian Networks and Neural networks are very strong machine learning tools but at the same time they are conceptually different. Modern Neural networks in the recent last ten years surprised all researchers with their incomparable ability to recognize patterns. Their applicability to real life AI problems attracted the interest of many investors and companies. However, the way that they find solutions is a black box. Bayesian Networks on the other hand are very useful for medical problems where you want to build an expert model for diagnosis. Bayesian networks are conceptually different in the sense that they encapsulate the knowledge from data in variables that can be concepts of a domain expert. Furthermore, this is the only framework that can provide causal reasoning that explores causes and effects.

It is noted that all the works reviewed here concerning breast cancer diagnosis use thermography and BNs for classification only. No researcher utilizes the second big advantage of BNs: their ability to build a holistic expert model that can encapsulate certain and uncertain knowledge from AI classifiers from physicians from other tests etc. A BN expert model can integrate different diagnosis results coming from different AI techniques or other methods and suggest the final decision based on the utility theory.

## 5. Summary and Conclusion

A number of studies were conducted to identify whether thermography could be employed as a reliable tool to detect the breast tumor. Most of the studies agreed that thermography has potentials to be a noninvasive, safe and reliable tool for earlier breast cancer detection and prediction. However, at the present thermography could only be a supplementary tool for mammography, as it is very sensitive to the conditions of the procedure and wellness of the patient. Moreover, the main limitation of thermography is the weak surface signature of small and deep tumors. Notwithstanding, there is a renewed wave of interest in thermography because of the improvement of IR cameras sensors, though the development of such cameras still does not provide a more quantitative and robust procedure to detect the breast tumor.

On the other hand, the improvement of computer systems shows that mathematical modeling can also provide promising opportunities to improve the accuracy and reliability of tumor diagnosis. Numerical modeling of the tumor inside the breast is a complex process, at the same time it is a reliable one to supplement thermography and helps us to shift from qualitative to the quantitative assessment of the thermograms. Nonetheless, numerical methods and models can only be improved by validation against benchmark experimental data. Future research should focus on the development of sophisticated patient-specific models for precision prediction of all the thermal phenomena in the breast, employing personalized or patient-specific characteristics of the breast and its tissues. This can be achieved by carrying out reverse

thermal modeling using the healthy and diseased breast thermograms and breast 3D geometry as inputs. Furthermore, these models can be used to improve thermal contrast in the transient cooling with dynamic IR thermography for the breast. It is also suggested that future thermography should contain the 3D distributions of surface temperature using 3D breast geometries. It can further be modified with a multilayer tissue model for improved accuracy and in an effort towards personalized medicine for breast cancer. This level of accuracy is important for revealing the exact correlation between the characteristics of the tumor and its thermal signature.

Artificial intelligence is recognized as an effective tumor classification tool with high sensitivity and specificity. The most useful application of Artificial Intelligence is Machine Learning. There are many Machine Learning algorithms such as: Naïve Bayes, Support Vector Machine, Decision Tree, Relevance Vector Machine, Convolutional Neural Network and Artificial Neural Network. AI techniques show good levels of accuracy, sensitivity and specificity obtained in the conducted studies. However the main limitation of the conducted studies is the limited number of thermograms available to be used in the studies, therefore the low levels of the robustness of the results of the study. It should be noted that these methods are not used in clinics and hospitals, as further developments are required to combine thermography, physics-based modeling and data-driven computation to diagnose breast cancer. Physics Informed Neural Network (PINN) seems to be an ideal method for such integration. Note also, that BNs can be the final layer that encapsulates and integrates in a mathematical consistent way, the knowledge coming from thermal modeling from various medical tests, from patient history profile, from experts and from one or more AI diagnostic methods/tools towards the final diagnosis decision.

For future studies, it is recommended to have publicly available standardized image databases, which include images from different modalities for similar cases in order to facilitate the tasks of classification based on the machine learning, data-driven simulation and physics-based modeling.

### Acknowledgement

The authors are grateful to the Ministry of Education and Science of the Republic of Kazakhstan for financing this work through the grant financing under the project “Application of artificial intelligence to complement thermography for breast cancer prediction” (AP08857347) and Nazarbayev University for administering the research project.

### References

1. *Infrared Imaging technology for breast cancer detection - Current status, protocols and new directions.* **S.G. Kandlikar, I. Perez-Raya, P.A. Raghupathi, J.S. Gonzalez-Hernandez, D. Dabydeen, L. Medeiros, P. Phatak.** s.l. : International Journal of heat and mass transfer, 2017, Vol. 108, pp. 2303-2320.
2. *The causes of cancer: quantitative estimates of avoidable risks of cancer in the United States today.* **R. Doll, R. Peto.** Cancer, USA : J. Natl. Cancer Inst., 1981, J. Natl. Cancer Inst., Vol. 66(6), pp. 1192-1208.
3. *The causes and prevention of cancer.* **B.N. Ames, L.S. Gold, W.C. Willett.** Cancer, Washington, DC : <https://doi.org/10.1073/pnas.92.12.5258>, 1995, Proc. Natl. Acad. Sci., Vol. 92(12), pp. 5258-5265.
4. **Institute, National Cancer.** National Cancer Institute. [Online] NIH Turning Discovery Into Health. [Cited: August 2, 2020.] <https://www.cancer.gov/types/breast/patient/breast-treatment-pdq#section/all>.
5. *World Health Organization (2021). Breast Cancer.* Retrieved from <https://www.who.int/news-room/fact-sheets/detail/breast-cancer>
6. *Projections of the cost of cancer care in the United States 2010-2020.* **A.B. Mariotto, K.R. Yabroff, Y. Shao, E.J. Feuer, M.I. Brown.** 2011, JNCI J. Natl. Cancer Inst, Vol. 103(2), pp. 117-128.
7. *An improved three-dimensional direct numerical modelling and thermal analysis of a female breast with tumour.* **E.Y.K. Ng, N.M. Sudharsan.** 2001, Proc. Inst. Mech. Eng., Vol. 215 (1), pp. 25-37.
8. *Functional infrared imaging of the breast.* **J.R. Keyserlingk, P.D. Ahlgren, E. Yu, N. Belliveau, M. Yassa.** 2000, IEEE Eng. Med. Biol. Mag., Vol. 19 (3), pp. 30-41.

9. *Relationship between microvessel density and thermographic hot areas in breast cancer.* **T. Yahara, T. Koga, S. Yoshida, S. Nakagawa, H. Deguchi, K. Shirouzu.** 2003, Surg. Today, Vol. 33 (4), pp. 243-248.
10. *2016 International Conference on Advances in Computing, Communications and Informatics, ICACCI 2016.* **S. Pramanik, D. Bhattacharje, M. Nasipuri.** 2016. Texture analysis of breast thermogram for differentiation of malignant and benign breast. pp. 8-14.
11. *Supportive Noninvasive Tool for the Diagnosis of Breast Cancer Using a Thermographic Camera Sensor.* **M.A. Garduno-Ramon, S. G. Vega-Mancilla, L.A. Morales-Henandez, R.A. Osornio-Rios.** s.l. : doi:10.3390/s17030497, 2017, Sensors, Vol. 17, p. 497.
12. *Breast thermography and cancer risk prediction.* **Gautheria M., Gros C.M.** 1980, Cancer, Vol. 45, pp. 51-56.
13. *Computerized breast thermography: Study of image segmentation and temperature cyclic variations.* **Ng E.Y.K., Chen Y., Ung L.** 2001, J. Med. Eng. Technol., Vol. 25, pp. 12-16.
14. *Bjurstam N., Hedberg K., Hultborn K., Johansson N., Johnsen C. Diagnosis of breast carcinoma. In progress in surgery.* London : Karger Publishers, 1974. pp. 1-65.
15. *The radiation of heat from the human body. I. An instrument for measuring the radiation and surface temperature of the skin .* **Hardy, J. D.** 1934, J. Clin. Invest., Vol. 13, pp. 593-604.
16. *"The radiation of heat from the human body. II. A comparison of some methods of measurement," .* **Hardy, J. D.** 1934, J. Clin. Invest., Vol. 13, pp. 605-614.
17. *"The radiation of heat from the human body. III. The human skin as a black-body radiator,".* **Hardy, J.D.** 1934, J. Clin. Invest., 13 615 –620 (1934), Vol. 13, pp. 615-620.
18. *The radiation of heat from the human body. IV. The emission, reflection, and transmission of infrared radiation by the human skin.* **J. D. Hardy, C. Muschenheim.** 1934, J. Clin. Invest., Vol. 13, pp. 817-831.
19. *The radiation of heat from the human body. V. The transmission of infra-red radiation through skin .* **J. D. Hardy, C. Muschenheim.** 1935, J. Clin. Invest., Vol. 14, pp. 1-9.
20. *Goniometric spectrometer for the measurement of diffuse reflectance and transmittance of skin in the infrared spectral region .* **C. Clark, R. Vinegar, J. D. Hardy.** 1953, J. Opt. Soc. Am., Vol. 43, pp. 993-998.
21. *Spectral transmittance and reflectance of excised human skin.* **J. D. Hardy, H. T. Hammel, D. Murgatroyd.** 1956, J. Appl. Physiol., Vol. 9, pp. 257-264.
22. *Automatic recording reflectometer for measuring diffuse reflectance in the visible and infrared regions.* **W. L. Derksen, T. I. Monahan, A. J. Lawes.** 1957, J. Opt. Soc. Am., Vol. 47, pp. 995-999.
23. *Measurement of the total normal emissivity of skin without the need for measuring skin temperature.* **D. Mitchell, T. Hodgson, F. R. N. Nabarro.** 1967, Phys. Med. Biol., , Vol. 12, pp. 359-366.
24. *The calculation of the emissivity of cylindrical cavities giving near black-body radiation.* **Quinn, T. J.** 1967, Br. J. Appl. Phys., Vol. 18, pp. 1105-1113.
25. *Wavelength dependence of skin emissivity.* **Watmough, D.J.** s.l. : Phys. Med. Biol., 1969, Vol. 14, pp. 201-204.
26. *Spectral emissivity of skin and pericardium .* **Steketee, J.** 1973, Phys. Med. Biol., Vol. 18, pp. 686-694.
27. *Foundations of thermometry.* **T. J. Quinn, J. P. Compton.** 1975, Rep. Prog. Phys., Vol. 38, pp. 151-239.
28. **Pratt, W. K.** *Digital Image Processing.* New York : John Wiley & Sons, 1978. pp. 1-24.
29. *The optics of human skin.* **R. R. Anderson, J. A. Parrish.** 1981, J. Invest. Dermatol., Vol. 77, pp. 13-19.
30. *Implications of surface temperatures in the diagnosis of breast cancer.* **Lawson, R.** 1956, Can. Med. Assoc. J., Vol. 75 (4), pp. 309-310.
31. *Breast cancer and body temperature.* **R. Lawson, M.S. Chughtai.** 1963, Can. Med. Assoc. J., Vol. 88(2), pp. 68-70.
32. *Thermopathology of breast cancer: measurement and analysis in vivo temperature and blood flow.* **Gautherie, M.** 1980, Ann. N. Y. Acad. Sci. , Vol. 335 (1), pp. 383 - 415.

33. *Thermographic localization of incompetent perforating veins in the leg.* **K.D. Patil, J.R. Williams, K.L. Williams.** 1970, Br. Med. J., Vol. 1 (5690), pp. 195-197.
34. *Detection of breast cancer by liquid crystal thermography. A preliminary report.* **T.W. Davision, K.L. Ewing, J. Ferguson, M. Chapman, A. Chan, C.C. Voorhis.** 1972, Cancer, Vol. 29 (5), pp. 1123-1132.
35. *On the feasibility of obtaining three dimensional information from thermographic measurements.* **M.M. Chen, C.O. Pederson, J.C. Chato.** 1977, Journal of Biomechanical Engineering, pp. 58-64.
36. *An analytical model of the countercurrent heat exchange phenomena.* **J.W. Mitchell, G.E. Myers.** 1968, Biophys. J., Vol. 8, pp. 897-911.
37. *Breast thermography after four years and 10,000 studies.* **J.H. Isard, W. Becker, R. Shilo, B.J. Ostrum.** 1972, American Journal of Roentgenology and Nuclear Medicine, Vol. 115(4), pp. 811-821.
38. *Thermogram aided clinical examination of the breast - an Alternative to Mammography for women 50 and younger.* **O.T. Siu, W.R. Ghent, B.T. Colwell, J.C. Henderson.** 1982, Canadian Journal of Public Health, Vol. 73(4), pp. 232-235.
39. *An analysis of peripheral heat transfer in man.* **K.H. Keller, L. Seiler.** 1971, J. Appl. Physiol., Vol. 30(5), pp. 779-786.
40. *Microvascular contributions in tissue heat transfer.* **M.M. Chen, K.R. Holmes.** 1980, Ann. N.Y. Acad. Sci., Vol. 335, pp. 137-151.
41. *Heat transfer of blood vessels.* **Chato, J.** 1980, J. Biomech. Eng.-Trans. ASME, Vol. 102(2), pp. 110-118.
42. *Temperature and blood flow patterns in breast cancer during natural evolution and following radiotherapy.* **Gautherie, M.** 1982, Biomedical Thermology, pp. 21-64.
43. *Indirect signs of breast cancer: Angiogenesis Study.* **Gamagami, P.** s.l. : Atlas Mammogr, 1996.
44. *Thermobiological assessment of benign and malignant breast diseases.* **Gautherie, M.** 1983, Am. J. Obstet. Gynecol., Vol. 147(8), pp. 861-869.
45. *A review of thermography as promising non-invasive detection modality for breast tumors.* **Ng, E.Y.K.** 2009, Int. J. Therm. Sci., Vol. 48(5), pp. 849-859.
46. *Analysis of transient thermal processes for improved visualization of breast cancer using IR imaging .* **M. Kaczmarek, A. Nowakowski.** 2003, Proceedings of the 25-th Annual International Conference of the IEEE Engineering in Medicine and Biology Society, Vol. 2, pp. 1113-1116.
47. *Advantages of subtraction thermography in the diagnosis of breast disease.* **H. Usuki, S. Teramoto, S. Komatsubara, S.I. Hirai, T. Misumi, M. Murakami, Y. Onoda, K. Kawashima, K. Kino, K.I. Yamashita, J. Matsubara.** 1991, Biomedical Technology, Vol. 11(4), pp. 286-291.
48. *Breast Thermal Imaging: The paradigm shift.* **Cockburn, W.** 1995, Thermologie Oesterreich, Vol. 5, pp. 49-53.
49. **J. Mooibroek, J. Crezee, J. Lagendijk.** *Basic of thermal models: thermoradiotherapy and Thermochemotherapy.* Berlin : Springer, 1995. pp. 425-433.
50. *Analysis of tissue and arterial blood temperatures in the resting human forearm.* **Pennes, H.H.** 1948, J. Appl. Physiol., Vol. 85(1), pp. 93-122.
51. *Influence of blood supply on thermal properties and metabolism of mammary carcinomas .* **Gullino, P.M.** 1980, Ann. N. Y. Acad. Sciences, Vol. 335, pp. 1-21.
52. *Applying dynamic thermography in the diagnosis of breast cancer.* **Y. Ohashi, I. Uchida.** 2000, IEEE Eng. Med. Biol. Mag, Vol. 19(3), pp. 42-51.
53. *The role of dynamic infrared imaging in melanoma diagnosis.* **Herman, C.** 2013, Expert Rev. Dermatol., Vol. 8(2), pp. 177-184.
54. *Modeling static and dynamic thermography of the human breast under elastic deformation.* **L. Jiang, W. Zhan, M.H. Loew.** 2011, Phys. Med. Biol., Vol. 56(1), p. 187.
55. *Effect of forced convection on the skin thermal expression of breast cancer .* **L. Hu, A. Gupta, J.P. Gore, L.X. Xu.** 2004, J. Biomech. Eng., Vol. 126(2), p. 204.
56. *Breast thermography. A prognostic indicator for breast cancer survival.* **J.H. Isard, C.J. Sweitzer, G.R. Edelstien.** 1988, Cancer, Vol. 62, pp. 484-488.



57. *Breast thermography is a noninvasive prognostic procedure that predicts tumor growth rate in breast cancer patients.* **J.F. Head, F. Wang, R.L. Elliott.** 1993, Ann. N. Y. Acad. Sci., Vol. 698(1), pp. 153-158.
58. *Angiogenesis in preinvasive lesions of the breast.* **A.J. Guidi, S.J. Schnitt.** 1996, Breast J., Vol. 2(6), pp. 364-369.
59. *Comparison of the accuracy of thermography and mammography in the detection of breast cancer.* **R. Omranipour, A. Kazemian, S. Alipour, M. Najafi, M. Alidoosti, M. Navid, A. Alikhassi, N. Ahmadinejad, K. Bagheri, S. Izadi.** 2016, Breast Care, Vol. 11(4), pp. 260-264.
60. **Administration, U.S. Food and Drug.** U.S. Food and Drug Administration. [Online] [Cited: August 2, 2020.] <https://www.fda.gov/medical-devices/safety-communications/fda-warns-thermography-should-not-be-used-place-mammography-detect-diagnose-or-screen-breast-cancer>.
61. *The energy conservation equation for living tissue.* **Wulff, W.** 1974, IEEE Trans. Biomed. Eng BME, Vol. 21(6), pp. 494-495.
62. *Theory and experiment for the effect of vascular microstructure on surface tissue heat transfer. Part I: Anatomical foundation and model conceptualization .* **S. Weinbaum, L.M. Jiji, D.E. Lemons.** 1984, J. Biomech. Eng. , Vol. 106(4), pp. 321-330.
63. *Theory and experiment for the effect of vascular microstructure on surface tissue heat transfer - Part II: Model formulation and solution.* **S. Weinbaum, L.M. Jiji, D.E. Lemons.** 1984, J. Biomech. Eng., Vol. 106(4), pp. 331-341.
64. *A new simplified bioheat equation for the effect of blood flow on local average tissue temperature.* **S. Weinbaum, L.M. Jiji.** 1985, J. Biomech. Eng. , Vol. 107 (2), pp. 131-139.
65. *On the generalization of the Weinbaum-Jiji bioheat equation to microvessels of unequal size; the relation between the near field and local average tissue temperatures.* **M. Zhu, S. Weinbaum, L.M. Jiji, D.E. Lemons.** 1988, J. Biomech. Eng., Vol. 110(1), pp. 74-81.
66. *The matching of thermal fields surrounding countercurrent microvessels and the closure approximation in the Weinbaum-Jiji equation.* **S. Weinbaum, L.M. Jiji.** 1989, J. Biomech. Eng., Vol. 111(4), pp. 271-275.
67. *An evaluation of the Weinbaum-Jiji bioheat equation for normal and hyperthermic conditions.* **C.K. Charny, S. Weinbaum, R.L. Levin.** 1990, J. Biomech. Eng. , Vol. 112(1), pp. 80-87.
68. *The bleed off perfusion term in the Weinbaum-Jiji bioheat equation .* **S. Weinbaum, L.M. Jiji, D.E. Lemons.** 1992, J. Biomech. Eng., Vol. 114(4), pp. 539-542.
69. *A new fundamental bioheat equation for muscle tissue: Part I - Blood perfusion term.* **S. Weinbaum, L.X. Xu, L. Zhu, A. Ekpene.** 1997, J. Biomech. Eng., Vol. 119(3), pp. 278-288.
70. *Bioheat transfer in a branching countercurrent network during hyperthermia.* **C.Charny, R. Levin.** 1989, J. Biomech. Eng.-Trans. Asme, Vol. 111(4), pp. 413-422.
71. *Advanced integrated technique in breast cancer thermography.* **E.Y.K. Ng, E.C. Kee.** 2008, J. Med. Eng. Technol. , Vol. 32(2), pp. 103-114.
72. *Numerical computation as a tool to aid thermographic interpretation .* **E.Y.K. Ng, N.M. Sudharsan.** 2001, J. Med. Eng. Technol. , Vol. 25(2), pp. 53-60.
73. *Finite element modelling for the detection of breast tumors.* **O. Mukhmetov, D. Igali, Y. Zhao, S. Ch. Fok, L. Teh, E.Y.K. Ng, A. Mashekova.** Taichung, Taiwan : s.n., 2018. Proceedings - 2018 IEEE 18-th International Conference on Bioinformatics and Bioengineering, BIBE. pp. 360-363.
74. *Thermal modeling of the normal woman's breast.* **M.M. Osman, E.M. Afify.** 1984, ASME Journal of Biomechanical Engineering, Vol. 106, pp. 123-130.
75. *Thermal modeling of the malignant woman's breast .* **M.M. Osman, E.M. Afify.** 1988, ASME Journal of Biomechanical Engineering, Vol. 110, pp. 269-276.
76. *Parametric optimization for tumor identification bioheat equation using ANOVA and the Taguchi Method.* **N.M. Sudharsan, E.Y.K. Ng.** 2000, Proc Instn Mech Engrs, Vols. 214, Part H, pp. 505-512.
77. *Effect of blood flow, tumour and cold stress in a female breast: novel time accurate computer simulation.* **E.Y.K. Ng, N.M. Sudharsan.** 2001, Proc Instn Mech Engrs, Vol. 215 (Part H).
78. *Thermal simulation of breast tumors.* **Gonzalez, F.J.** 2007, REVISTA MEXICANA DE FI'SICA, Vol.

53(4), pp. 323-326.

79. *Estimation of breast tumor thermal properties using infrared images.* **L.A. Bezerra, M.M. Oliveira, T.L. Rolim, A. Conci, F.G.S. Santos, P.R.M. Lyra, R.C.F. Lima.** 2013, Signal Processing, Vol. 93, pp. 2851-2863.

80. *Estimation of tumor characteristics in a breast tissue with known skin surface temperature.* **K. Das, S.C. Mishra.** 2013, J. Therm. Biol., Vol. 38(6).

81. *Simultaneous estimation of size, radial and angular locations of a malignant tumor in a 3-D human breast - numerical study.* **K. Das, S.C. Mishra.** 2015, Journal of Thermal Biology, Vol. 52, pp. 147-156.

82. *Potentialities of steady-state and transient thermography in breast tumour depth detection: a numerical study.* **A. Amri, S.H. Pulko, A.J. Wilkinson.** 2016, Comput. Methods Programs Biomed., Vol. 123. 68-80.

83. *Tumor parameter estimation considering the body geometry by thermography.* **Sh. Hossain, F.A. Mohammadi.** 2016, Computers in Biology and Medicine, Vol. 76, pp. 80-93.

84. *Parameter estimation of breast tumour using dynamic neural network from thermal pattern.* **E. Saniei, S. Setayeshi, M.E. Akbari, M. Navid.** 2016, Journal of Advanced Research, Vol. 7, pp. 1045-1055.

85. **Y. Zhao, A. Mashekova, O. Mukhmetov.** *Scientific report. Development of an intellectual system for early detection of breast tumors and prediction of breast cancer development.* Nur-Sultan : National center of science and technology evaluation, 2019. No. APO5130923.

86. *Surface temperature distribution of a breast with and without tumour.* **N.M. Sudharsan, E.Y.K. Ng, S.L. Teh.** 1999, Comput Methods Biomech. Biomed. Engin., Vol. 2(3), pp. 187-199.

87. *Analytical Solutions of Pennes Bioheat Transfer equation with a Blood Vessel.* **H.W. Huang, C.L. Chan, R.B. Roemer.** 1994, J. Biomech. Eng, Vol. 116(2), pp. 208-212.

88. *Lattice Boltzmann method for solving the bioheat equation.* **Zhang, H.** 2008, Physics in Medicine and Biology, Vol. 53(3), pp. 15-23.

89. *Dimensionless solutions and general characteristics of bioheat transfer during thermal therapy .* **J. Okajima, Sh. Manuyama, H. Takeda, A. Komiya.** 2009, Vol. 34(8), pp. 377-384.

90. *Numerical simulation for heat transfer in tissues during thermal therapy.* **P.K. Gupta, J. Singh, K.N. Rai.** 2010, Journal of Thermal Biology, Vol. 35(6), pp. 295-301.

91. *Thermal analysis of a three-dimensional breast model with embedded tumour using the model with embedded tumour using the transmission line matrix (TLM) method.* **A. Amri, A. Saidane, S.H. Pulko.** 2011, Comput. Biol. Med., Vol. 41, pp. 76-86.

92. *Technology, application and potential of dynamic breast thermography for the detection of breast cancer.* **J.L. Gonzalez-Hernandez, A.N. Recinella, S.G. Kandlikar, D. Dabydeen, L. Medeiros, P. Phatak.** 2019, International Journal of Heat and Mass Transfer, Vol. 131, pp. 558-573.

93. *International Mechanical Engineering Congress and Exposition.* **A. Channugam, R. Hatwar, C. Herman.** Houston, Texas, USA : ASME 2012 International Mechanical Engineering Congress and Exposition, 2012. Thermal analysis of cancerous breast model. Vol. Volume 2: Biomedical and Biotechnology, pp. 135-143. ISBN: 978-0-7918-4518-9.

94. *Medical Imaging 2011: Biomedical Applications in Molecular, Structural, and Functional Imaging.* **L. Jiang, W. Zhan, M.H.Loew.** [ed.] Robert C. Molthen John B. Weaver. 2011. Toward understanding the complex mechanisms behind breast thermography: an overview for comprehensive numerical study. Vols. 7965, 79650H, p. 187. doi: 10.1117/12.877839.

95. *Inverse method for quantitative characterisation of breast tumour from surface temperature data .* **R. Hatwar, C. Herman.** 2017, Int. J. Hyperthermia, Vol. 33 (7), pp. 741-757.

96. *Breast tumor simulation and parameters estimation using evolutionary algorithms.* **M.Mital, R.M. Pidaparti.** 2008, Model Simul Eng, Vol. Special Issue, p. 6 pages.

97. *A neural network based estimation of tumour parameters from a breast thermogram.* **S. Mitra, C. Balaji.** 2010, Int J Heat Mass Tran, Vol. 53, pp. 2851-63.

98. *Identification of tumor region parameters using evolutionary algorithm and multiple reciprocity boundary element method.* **M. Parush, E. Majchrzak.** 2007, Eng Appl Artif Intell, Vol. 20(5), pp. 647-

655.

99. *Tumor location and parameter estimation by thermography.* **J.P. Agnelli, A.A. Barrea, C.V. Turner.** 2011, Math Comput Model, Vols. 53 (7-8), pp. 1527-1534.

100. *Shape optimization for tumor location.* **J.P. Agnelli, C. Padra, C.V. Tumer.** 2011, Comput Math Appl, Vol. 62(11), pp. 4068-4081.

101. *Procedure to estimate thermophysical and geometrical parameters of embedded cancerous lesions using thermography.* **J.M. Luna, R. Romero-Mendez, A. Hemandez-Guerrero, F. Elizalde-Blancas.** 2012, J. Biomech. Eng., Vol. 134(3).

102. *Clinical breast cancer analysis with surface fitting in the medical thermal texture maps.* **F. Ye, G.L. Shi.** 2012, Appl Mech Mater, pp. 263-266.

103. *Morphological measurement of localized temperature increases amplitudes in breast infrared thermograms and its clinical application.* **X. Tang, H. Ding, Y. Yuan, Q. Wang.** 2008, Biomed. Signal Process. Control, Vol. 3(4), pp. 312-318.

104. *Pattern recognition approaches for breast cancer DCE-MRI classification: a systematic review.* **R. Fusco, M. Sansone, S. Filice, G. Carone, D.M. Amato, C. Sansone, A. Petrillo.** 2013, J. Med. Biol. Eng., Vol. 36(4), pp. 449-459.

105. *Anniversary paper: history and status of CAD and quantitative image analysis: the role of medical physics and AAPM.* **M.L. Giger, H.P. Chan, J. Boone.** 2008, Med. Phys., Vol. 35(12), pp. 5799-5820.

106. *Computer-aided detection/diagnosis of breast cancer in mammography and ultrasound: a review.* **A. Jalalian, S.B. Mashohor, H.R. Mahmud, M.I. Saripan, A.R. Ramli, B. Karasfi.** 2013, Clin. Imaging, Vol. 37(3), pp. 47-51.

107. **J. Han, M. Kamber, J. Pei.** *Data mining: Concepts and techniques.* Oxford : Elsevier, 2012.

108. *Breast cancer diagnosis by using k-nearest neighbors with different distances and classification rules.* **S.A. Medjahed, T.A. Saadi, A. Benyettou.** 2013, Int. J. Com-put. Appl., Vol. 62(1), pp. 1-5.

109. *Artificial Neural Networks in Medical Diagnosis.* **F. Amato, A. Lopez-Rodriquez, E.M. Pena-Mendez, P. Vanhara, A. Hampl, J. Havel.** 2013, Journal of Applied Biomedicine, Vol. 11(2), pp. p. 47-58.

110. *Feed forward artificial neural network: tool for early detection of ovarian cancer.* **A. Thakur, V. Mishra, S.K. Jain.** 2011, Sci. Pharm, Vol. 79(3), pp. 493-506.

111. *Classification of breast cancer using gene index based fuzzy supervised learning in guest decision tree algorithm.* **P. Bethapudi, E.S. Reddy, K.V. Varma.,** 2015, Int. J. Comput. Appl., Vol. 111(14), pp. 50-57.

112. *Proceedings of the Ninth Australasian Data Mining Conference.* **M. Shouman, T. Turner, R. Stocker.** s.l. : Australian Computer Society, Inc., 2011. Using decision tree for diagnosing heart disease patients. Vol. 121.

113. *Hybrid feature selection based weighted least squares twin support vector machine approach for diagnosing breast cancer, hepatitis and diabetes.* **D.Tumor, S. Agarwal.** 2015, Adv. Artif. Neural Syst., Vol. 2015.

114. *The method and efficacy of support vector machine classifiers based on texture features and multi-resolution histogram from 18 F-FDG PET-CT images for the evaluation of mediastinal lymph nodes in patients with lung cancer.* **X.Gao, C.Chu, Y.Li, P.Lu, W.Wang, W.Liu, L.Yu.** 2015, Eur. J. Radiol., Vol. 84(2), pp. 312-317.

115. *Advanced infrared image processing for breast cancer risk assessment.* **C.A. Lipari, J.F. Head.** Chicago : The 19-th Annual International Conference of the IEEE Engineering in Medicine and Biology Society, 1997. Advanced infrared image processing for breast cancer risk assessment. Vol. 2, pp. 673-676.

116. *Computerized image analysis of digitized infrared images of breasts from a scanning infrared image system.* **J.F. Head, C.A. Lipari, R.L. Elliot.** s.l. : The International Society for Optical Engineering, 1998, Proceedings of SPIE, Vol. 3436, pp. 290-294.

117. *Asymmetric analysis using automatic segmentation and classification for breast cancer detection in thermograms.* **H. Qi, J.F. Head.** s.l. : Proceedings of the 23rd Annual International Conference of the IEEE



- Engineering in Medicine and Biology Society, 2001. Asymmetric analysis using automatic segmentation and classification for breast cancer detection in thermograms. Vol. 3, pp. 2866-2869.
118. *24th Annual Conference and the Annual Fall Meeting of the Biomedical Engineering Society EMBS/BMES Conference*. **P.T. Kuruganti, H. Qi**. s.l. : Engineering in Medicine and Biology, 2002. Assymetri analysis in breast cancer detection using thermal infrared images, . Vol. 2, pp. 1155-1156.
119. *Targeting breast cancer detection with military technology*. **Irvine, J.M.** 2002, IEEE Eng. Med. Biol. Mag., Vol. 21(6), pp. 36-40.
120. *Thermal signatures for breast cancer screening comparative study*. **T. Jakubowska, B. Wiecek, M. Wysocki, C. Drews-Peszynski**. 2003. Proceedings of the 25-th Annual International Conference of the IEEE Engineering in Medicine and Biology Society. Vol. 2, pp. 1117-1120.
121. *Evaluation of the diagnostic performance of infrared imaging of the breast: a preliminary study*. **J. Wang, K.J. Chang, C.Yu Chen, K.L. Chien, Yu Sh. Tsai, Y.M. Wu, Yu Ch. Teng, T. Ting-Fang Shih**. 2010, Biomed. Eng. Online, Vol. 9, p. 3.
122. *Thermography based breast cancer analysis using statistical features and fuzzy classification*. **G. Schaefer, M. Zavissek, T. Nakashima**. 2009, Pattern Recognit., Vol. 42, pp. 1133-1137.
123. *Segmentation of breast thermogram images for the detection of breast cancer - A projection profile approach*. **K.Prasad, K. Rajagopal**. 2015, J. Image Graph, Vol. 3, pp. 47-51.
124. *An infrared image based methodology for breast lesions screening*. **K.C.C. Morais, J.V.C. Vargas, G.G. Reiserberger, F.N.P. Freitas, S.H. Oliari, M.L. Brioschi, M.H. Louveira, C. Spautz, F.G. Dias, P. Gasperin, V.M. Budel, R.A.G. Cordeiro, A.P.P. Schittini**. 2016, Infrared Physics & Technology, Vol. 76, pp. 710-721.
125. **K. Ito, A.W. Asnido, S.A. Daud, E.Y.K. Ng**. Thermal analysis on 3D breast cancer model. *Computational modelling and simulation for biomedical applications*. s.l. : Penerbit UTM Press, Vol. Ch 9.
126. *Tumor localization in breast thermography with various tissue compositions by using Artificial Neural Network*. **A.A. Wahab, M.I. Mohamad Salim, J. Yunus, M.N. Che Aziz**. 2015. 2015 IEEE Student conference on Research and Development . pp. 484-488.
127. **Lab, Visual**. Visual Lab. [Online] [Cited: June 7, 2020.] <http://visual.ic.uff.br/en/proeng/>.
128. Physics-informed neural networks: A deep learning framework for solving forward and inverse problems involving nonlinear partial differential equations. **M. Raissia, P. Perdikaris, G.E. Karniadakis**. 2019, Journal of Computational Physics, Vol. 378, pp. 686–707.
129. Physics-Informed Neural Networks (PINNs) for Heat Transfer Problems. **S.Z. Cai, Z.C. Wang, S.F. Wang, P. Perdikaris, G.E. Karniadakis**. 2021, Journal of Heat Transfer. Accepted manuscript posted March 17, 2021. doi:10.1115/1.4050542.
130. *Thermography based breast cancer detection using texture features and support vector machine*. **U.R. Acharya, E.Y.K. Ng, J.H. Tan, S.V. Sree**. 2010, Journal Med Syst, Vol. 36(3), pp. 1503-1510.
131. *Comparative study on the use of analytical software to identify the different stages of breast cancer using discrete temperature data*. **J.M.Y. Tan, E.Y.K Ng, U.R. Acharya, L.G. Keith, J. Holmes**. 2008, J Med Syst, Vol. 33(2), pp. 141-153.
132. *An Integrated Index for Breast Cancer Identification using Histogram of Oriented Gradient and Kernel Locality Preserving Projection Features Extracted from thermograms*. **U. Raghavendra, U.R. Acharya, E.Y.K. Ng, Jen-HongTan, Z. Anjan Gudikar**. 2016, Quantitative Infrared Thermography Journal, Vol. 13(2), pp. 195-209.
133. *Breast cancer risk detection using RVM*. **B.M. Gayathi, C.P. Sumathi**. 2015, International Journal of Applied Engineering Research, Vol. 10 (5), pp. 3979-3982.
134. *Evaluating the efficiency of infrared breast thermography for early breast cancer risk prediction in asymptomatic population*. **U.R. Gogoi, G. Majumdar, M.K. Bhowmik, A.K. Ghosh**. 2019, Infrared Physics & Technology, Vol. 99, pp. 201-211.
135. *Cancer classification using relevance vector machine learning*. **A. Bharathi, K. Anandakumar**.

- 2015, Journal of medical imaging and health informatics, Vol. 5(3), pp. 630-634.
136. *Kernel based relevance vector machine for cancer classification of diseases*. **E.Tcheimegni**. s.l. : Bowie state university, 2013, Vol. 202.
137. *Cancer classification using support vector machines and relevance vector machines based on Analysis of Variance features*. **A.Bharathi, A.M. Natarajan**. 2011, Journal of computer science, Vol. 7 (9), pp. 1393-1399.
138. *Breast cancer diagnosis and recurrence prediction using machine learning techniques*. . **M.Rana**. 2015, International journal of research in Engineering and Technology , Vol. 4 (4), pp. 372-376.
139. *Random forest classifier combined with feature selection for breast cancer diagnosis and prognostic*. . **C. Nguyen, Y. Wang, N, Nguyen**. 2013, Journal of Biomedical Science and Engineering, Vol. 6, pp. 551-560.
140. *The accuracy of digital infrared imaging for breast cancer detection in women undergoing breast biopsy*. **al., G.C. Wishart et**. 2010, Eur. J. Surg. Oncol. EJSO x, Vol. 36 (6), pp. 535-540.
141. *Evaluation of the diagnostic power of thermography in breast cancer using Bayesian Network Classifiers*. **C.R. Nicandro, M.M. Efren, A.A. Maria Ysaneli, M.D.C.M. Enrique, A. M. Hector Gabriel, P.C. Nancy, G.H. Alejandro, H.R. Guillermo De Jesus, B.M. Rocio Erandi**. s.l. : Computational and Mathematical Methods in Medicine, 2013, p. doi:10.1155/2013/264246.
142. *Assessment of Bayesian Network Classifiers as tools for Discriminating Breast Cancer Pre-Diagnosis based on three diagnostic methods*. **M.Y. Ameca-Alducin, N. Cruz-Ramirez, E. mezure-Montes, E. Martin-Del-Campo-Mena, N. Perez-castro, H.G. Acosa-Mesa**. s.l. : Lecture notes in computer science (including subseries lecture notes in artificial intelligence and lecture notes in bioinformatics), 2013, Vol. 7269 LNAI. doi:10.1007/978-3-642-37807-2\_36.
143. *Thermography based breast cancer detection using texture features and minimum variance quantization*. **M. Milosevic, D. Jankovic, A. Peulic**. 2014, EXCLI Journal, Vol. 13, pp. 1204-1215.
144. *Hybrid analysis for indicating patients with breast cancer using temperature time series*. **L.F. Silva, A.A.S.M.D. Santos, R.S. Bravo, A.C. Silva, D.C. Muchaluat-Saade, A.Conci**. 2016, Computer Methods and Programs in Biomedicine, Vol. 130, pp. 142-153. . doi:10.1016/j.cmpb.2016.03.002.
145. *Breast Cancer Diagnosis Based on Mammary Thermography and Extreme Learning Machines*. **M.A. de Santana, J.M.S. Pereira, F.L. da Silva, N.M. de Lima, F.N. de Sousa, G.M.S. de Arruda, R.C.F. de Lima, W.W.A. de Silva, W.P. dos Santos**. s.l. : Research on Biomedical Engineering, 2018, Vol. 34(1), pp. 45-53. doi:10.1590/2446-4740.05217.
146. *Breast Cancer Identification via Thermography Image Segmentation* . **S. Tello-Mijares, F. Woo, F. Flores**. 2019. doi:10.1155/2019/9807619.
147. *A finite element model of the breast for predicting mechanical deformations during biopsy procedures*. **F.S. Azar, D.N. Metaxas, M.D. Schnall**. 2000, IEEE Workshop on Mathematical Methods in Biomedical Image Analysis, pp. 38-45.
148. *Relationship between microvessel density and thermographic hot areas in breast cancer*. **T. Yahara, T. Koga, S. Yoshida, S. Nakagawa, H. Deguchi, K. Shirouzu**. 2003, Surg. Today , Vol. 33 (4), pp. 243-248.

**Declaration of interests**

☒ The authors declare that they have no known competing financial interests or personal relationships that could have appeared to influence the work reported in this paper.

☐ The authors declare the following financial interests/personal relationships which may be considered as potential competing interests: